

1 **On the similarity of hillslope hydrologic function: a clustering approach based**  
2 **on groundwater changes**

Deleted: function

Deleted: : a process-based approach

3  
4 Fadj Z. Maina<sup>1,2\*</sup>, Haruko M. Wainwright<sup>1</sup>, Peter James Dennedy-Frank<sup>1</sup>, Erica R. Siirila-  
5 Woodburn<sup>1</sup>

6 <sup>1</sup>Energy Geosciences Division, Lawrence Berkeley National Laboratory 1 Cyclotron Road, M.S.  
7 74R-316C, Berkeley, CA 94704, USA

8 <sup>2</sup>now at NASA Goddard Space Flight Center, Hydrological Sciences Laboratory, 8800 Greenbelt  
9 Rd, Greenbelt, 20771, MD, USA

10 \*Corresponding Author: fadjizaouna.maina@nasa.gov

13 **Abstract**  
 14 Hillslope similarity is an active topic in hydrology because of its importance to improve  
 15 our understanding of hydrologic processes and enable comparisons and paired studies. In this  
 16 study, we propose a holistic bottom-up hillslope clustering based on a region's integrative  
 17 hydrodynamic response quantified by the seasonal changes in groundwater levels  $\Delta P$ . The main  
 18 advantage of the  $\Delta P$  clustering is its ability to capture recharge and discharge processes. We test  
 19 the performance of the  $\Delta P$  clustering by comparing it to seven other common hillslope clustering  
 20 approaches. These include clustering approaches based on the aridity index, topographic wetness  
 21 index, elevation, land cover, and machine-learning that jointly integrate multiple data. We assess  
 22 the ability of these clustering approaches to identify and categorize hillslopes with similar static  
 23 characteristics, hydroclimate, land surface processes, and subsurface dynamics in a mountainous  
 24 watershed, the East River, located in the headwaters of the Upper Colorado River Basin. The  $\Delta P$   
 25 clustering performs very well in identifying hillslopes with 6 out of the 9 characteristics studied.  
 26 The variability among clusters as quantified by the coefficient of variation (0.2) is less in the  $\Delta P$   
 27 and the machine learning approaches than in the others (>0.3 for TWI, elevation, and land cover).  
 28 We further demonstrate the robustness of the  $\Delta P$  clustering by testing its ability to predict hillslope  
 29 responses to wet and dry hydrologic conditions, of which it performs well when based on average  
 30 conditions.

31 **Keywords:** Hillslope, similarity, seasonal groundwater variations, integrated hydrologic  
 32 modeling, hillslope clustering, hydrologic function

**Deleted:** similarity classification

**Deleted:** proposed

**Deleted:** classification

**Deleted:** describe

**Deleted:** proposed

**Deleted:** classification

**Deleted:** similarity

**Deleted:** classifications

**Deleted:** simple

**Deleted:** classifications

**Deleted:** more sophisticated

**Deleted:** classifications

**Deleted:** all these

**Deleted:** classifications

**Deleted:** ic behaviors

**Deleted:** proposed

**Deleted:** classification is robust as it reasonably identifies and categorizes hillslopes with similar elevation, land cover, hydroclimate, land surface processes, and subsurface hydrodynamics (and hence hillslopes with similar hydrologic function)

**Deleted:** (0.2)

**Deleted:** . In general, the other approaches are good in identifying similarity in a single characteristic, which is usually close to the selected variable.

**Deleted:** proposed

**Deleted:**

**Deleted:** classification

**Formatted:** Indent: First line: 0.5"

**Deleted:** classification

**Deleted:** function

**Deleted:** ¶

64

65 **1. Introduction**

66 The ability to delineate areas into spatially defined regions for their use in characterizing

67 hydrologic flow and transport behavior is important for several reasons, including the assessment,

68 monitoring, and modeling of water quantity and quality. Hillslopes are the scale at which

69 hydrologic flow and transport processes can be tractably and frequently measured. It is also the

70 scale at which flow and travel time are quantified, and the instrumentation, conceptualization, and

71 modeling of hydrologic processes occur (Fan et al., 2019, Wainwright et al., 2022). While

72 advancements have been made in the general understanding of hillslope dynamics over the last

73 several decades, there is yet to be a globally agreed-upon classification and/or clustering for this

74 important scale of interest in hydrology (McDonnell & Woods, 2004). Hydrologic signatures

75 within hillslopes are the results of several simultaneous and nonlinear above- and below-ground

76 processes. The uniqueness of a given location's characteristics (for example, the topography,

77 geology, vegetation, etc.) limits our ability to draw general hypotheses and to develop a similarity

78 framework (Beven, 2000). Nevertheless, a classification is needed to provide guidance on

79 catchments and hillslopes comparisons (McDonnell & Woods, 2004), paired studies (Andréassian

80 et al., 2012; Bosch & Hewlett, 1982; Brown et al., 2005), and improve our understanding of the

81 changes in hydrologic processes across the world. Further, hillslope similarity is potentially an

82 important step toward developing reduced-order models and machine learning algorithms, where

83 identifying regions based on their similarities can substantially reduce computational costs

84 (Chaney et al., 2018). The scaling of hillslope to catchment classifications can also be useful in

85 the prediction of hydrologic behavior in ungauged basins (Sivapalan et al., 2003), an exceedingly

86 important challenge.

Deleted: ¶

Deleted: ¶

Deleted: ¶

Formatted: Heading 1, Indent: Left: 0.75"

Deleted: water transfer

Deleted: quantified

Deleted:

Deleted: system

Deleted: By simplifying the complexities of the hydrologic dynamics, classification provides a better understanding of these processes.

Deleted: grouping

Deleted: grouping

Deleted: or dissimilarities

100 Hillslope similarity clustering approaches include the Topographic Wetness Index TWI  
101 (Beven & Kirby, 1979), which was proposed to quantify the topographic control on hydrology as  
102 topography plays a key role in the movement of water. Many other variants of this index have been  
103 later proposed to improve the definition of topographic similarity (Grabs et al., 2009; Hjerdt et al.,  
104 2004; Loritz et al., 2019). Other clustering approaches are based on hydroclimate (Carrillo et al.,  
105 2011), soil type and texture (Bormann, 2010), and land cover type (e.g., forest, urban, etc.  
106 (Wagener et al., 2007)). These indices assume that hillslopes with similar topography and land  
107 cover will have similar hydrologic responses. However, given that hydrologic processes are  
108 governed by many characteristics of the hillslope, clustering approaches relying on multiple  
109 landscape characteristics have also been proposed (Aryal et al., 2002; Sawicz et al., 2011). These  
110 top-down clustering approaches assume that areas with similar physical characteristics will lead  
111 to similar hydrologic processes (Oudin et al., 2010). Other clustering approaches use a bottom-up  
112 approach, where similarity is based on the hydrologic process. This clustering allows the  
113 estimation of the “hidden” hillslope characteristics such as soil texture, and geology that may drive  
114 similar hydrologic responses (Carrillo et al., 2011). Among the process-based clustering  
115 approaches existing in the literature we can cite: the Péclet number characterizing the diffusive  
116 and advective transfer of water at hillslope scale (Berne et al., 2005; S. W. Lyon & Troch, 2007;  
117 Steve W. Lyon & Troch, 2010) and the catchment seasonal water balance (Berghuijs et al., 2014).  
118 Other authors have derived hillslope similarities from subsurface flow dynamics (Harman &  
119 Sivapalan, 2009).

120 One challenge in developing a similarity framework is the inherent heterogeneity of a given  
121 hillslope. For example, Snow Water Equivalent (SWE), infiltration (I) and actual  
122 evapotranspiration (ET) distributions can range over an order of magnitude within a single

**Deleted:** Classical definitions of h

**Deleted:** classifications include similarities

**Deleted:** elevation

**Deleted:** similarity patterns

**Deleted:** based on the simultaneous accounting of multiple landscape characteristics. These classifications are mainly rely on usually based on clustering which aims to integrate all these data layers to identify and categorize similar hillslopes...

**Deleted:** classifications

**Deleted:** static

**Deleted:**

**Deleted:** and functions. This often-overlooked assumption presumes that an apparent physical similarity equates to a similarity in hydrologic processes

**Deleted:** classifications

**Deleted:** defined

**Deleted:** or functional response of interest

**Deleted:** A process-based classification enables the analysis of different hydrologic responses and the identification of the hydrologic function itself. It also

**Deleted:** classification

**Deleted:** hillslope

**Deleted:**

**Deleted:** can vary up to 300 mm; similarly, infiltration (I) and actual evapotranspiration (ET) rates

149 hillslope (Wainwright et al., 2022). Defining a single integrative measure that can capture this  
150 spatio-temporal variability is difficult. However, groundwater fluctuations are often tightly linked  
151 to seasonal changes in climate and have been shown to play an important role in surficial processes  
152 such as ET (Maina et al., 2022; Maina & Siirila-Woodburn, 2020; Maxwell & Condon, 2016).  
153 Thus, groundwater measures may serve as a good proxy for the aggregated hydrologic response.  
154 Groundwater dynamics could help overcome the issue of uniqueness of place because even if there  
155 are strong differences in the characteristics of the hillslope, the integrated response may be similar  
156 as some of the processes might not be important. Finally, the implications of groundwater changes  
157 are also important. For example, many regions are characterized by groundwater-dependent  
158 ecosystems or are hypothesized to have water table fluctuations affecting bedrock weathering rates  
159 and therefore the concentration and fluxes of metals and nutrients exports (e.g., Winnick et al.,  
160 2017).

Deleted: weather

161 In this study, we define a holistic bottom-up hillslope clustering using the integrative  
162 hydrologic response quantified by the seasonal changes in groundwater levels. A caveat to this  
163 clustering is that groundwater dynamics are difficult to quantify, and their measurements are  
164 frequently scarce. Hence, there are very few studies that use this variable to develop a hillslope  
165 similarity classification (Aryal et al., 2002; S. W. Lyon & Troch, 2007). However, today, thanks  
166 to advances in integrated hydrologic modeling (Brunner & Simmons, 2012; Maxwell & Miller,  
167 2005), accurate quantification of the groundwater dynamics at high resolution in both time and  
168 space, as well as their interaction with the key land surface processes and features, is now feasible.  
169 These models (e.g., HydroGeoSphere (Brunner and Simmons, 2012), ParFlow (Maxwell & Miller,  
170 2005), Advanced Terrestrial Simulator, (Coon et al., 2016)) that can be constrained with ground  
171 observations and measurements at ultra-high resolutions through aerial or remote sensing (i.e.,

Deleted: similarity framework based

Deleted: on a region's

Deleted: hydrodynamic

Deleted: , hereafter referred to as a region's *functional zonation*

Deleted: approach

Deleted: framework

Formatted: Font color: Text 1

180 drones, planes, or satellites) account for the two-way interactions between groundwater and land  
181 surface processes. Spatially resolved hydrologic flow models also enable us to jointly quantify  
182 other hydrologic variables useful to identify hillslope with similar hydrologic responses, namely  
183 trends in ET, SWE, and I. Nevertheless, we acknowledge that groundwater dynamics in some  
184 regions such as arid areas could be disconnected to land surface processes and less dependent to  
185 many key physical features of the hillslope, which may impede the ability of the proposed  
186 clustering in these regions.

**Deleted:** of interest

**Deleted:** . These variables may be useful to define functional zonation (i.e., areas with similar hydrologic functions) and can be constrained by measurements at ultra-high resolutions through aerial or remote sensing (i.e., drones, planes, or satellites)

**Deleted:** on

187 We test the proposed hillslope clustering on the site of the Department of Energy's (DOE)  
188 Watershed Function Scientific Focus Area (SFA) located in the headwaters of the Upper Colorado  
189 River Basin. The East River watershed is not only representative of many headwater catchments  
190 in the western United States in terms of its spatial heterogeneity of above and below-ground  
191 characteristics but also serves as an important proxy of water quantity and quality trends which  
192 ultimately impact a large population of water supply in the western United States, for municipal,  
193 agriculture, and industrial use (Hubbard et al., 2018). We test the robustness of the proposed  
194 hillslope clustering by comparing it to seven other common hillslope clustering approaches based  
195 on the aridity index (AI), TWI, elevation, land cover, and more sophisticated machine-learning  
196 approaches that jointly integrate multiple input data layers such as elevation, land cover, and  
197 geology, and model outputs including ET, and SWE. We assess the ability of these clustering  
198 approaches to identify and categorize hillslopes with similar physical characteristics (land cover  
199 and elevation), hydroclimate (precipitation and temperature), land surface processes (ET and  
200 SWE), subsurface dynamics (soil saturation, water table depth WTD, and seasonal changes in  
201 groundwater). We aim to provide answers to the following questions:

**Deleted:** similarity approach

**Deleted:** US

**Deleted:** (

**Deleted:** )

**Deleted:** The East River mountainous headwater catchment, characterized by high spatial and temporal variabilities in above-ground and below-ground hydrologic responses (Hubbard et al., 2018), is a good candidate site to demonstrate our approach.

**Deleted:** similarity framework

**Deleted:** similarity measures. These

**Deleted:** include approaches based on single data layers (

**Deleted:** and

**Deleted:** )

**Deleted:** approaches

**Deleted:** and

225 • What are the best clustering approaches for identifying hillslopes with similar  
226 hydrologic processes?

Deleted: classifications

Deleted: functions

227 • Is a similarity index based on the seasonal groundwater variations sufficient to  
228 capture all the complex processes taking place at a hillslope scale?

229

## 230 2. Methodology

### 231 2.1. Modeling framework

#### 232 2.1.1. Selected integrated hydrologic model: ParFlow-CLM

Deleted: s

Deleted: Numerical model

Formatted: Normal

Formatted: Heading 3 Char

Deleted: T

233 We use the integrated hydrologic model, ParFlow, which has the advantages of simulating  
234 the water and energy balance from the bedrock to the lower atmosphere and therefore connect  
235 groundwater dynamics with land surface processes. ParFlow solves the subsurface flow using the  
236 three-dimensional mixed form of the Richards equation (Richards, 1931) given by the following  
237 equation:

$$238 S_S S_W(\psi_P) \frac{\partial \psi_P}{\partial t} + \phi \frac{\partial S_W(\psi_P)}{\partial t} = \nabla \cdot [K(x) k_r(\psi_P) \nabla(\psi_P - z)] + q_s \quad (1)$$

239 Where is  $S_S$  the specific storage [ $L^{-1}$ ],  $S_W(\psi_P)$  is the degree of saturation [-] associated  
240 with the subsurface pressure head  $\psi_P$  [L],  $t$  is the time [T],  $\phi$  is the porosity [-],  $k_r$  is the relative  
241 permeability [-],  $z$  is the depth [L],  $q_s$  is the source/sink term [ $T^{-1}$ ] and  $K(x)$  is the saturated  
242 hydraulic conductivity [ $L T^{-1}$ ] which is assumed to be a diagonal tensor with entries given as:

243  $k_x(x)$ ,  $k_y(x)$  and  $k_z(x)$ . We assumed in this work that the domain is isotropic, and that the tensor  
244 is equal to 1 for all the three directions at each cell of the discretized model. In the unsaturated  
245 zone, both  $S_W$  and  $k_r$  depend on the  $\psi$ . The relationships between  $S_W$  and  $k_r$  and  $\psi$  are described  
246 by the van Genuchten model (van Genuchten, 1980).

247 Overland flow (equation 2) is solved by the kinematic wave equation in two dimensions.

$$248 -k(x) k_r(\psi_0) \nabla(\psi_0 - z) = \frac{\partial \|\psi_0, 0\|}{\partial t} - \nabla \cdot v \|\psi_0, 0\| - q_r(x) \quad (2)$$

254 Where  $\psi_0$  is the ponding depth,  $\|\psi_0, 0\|$  indicates the greater term between  $\psi_0$  and 0,  $v$  is  
 255 the depth averaged velocity vector of surface runoff [ $L T^{-1}$ ],  $q_r$  is a source/sink term representing  
 256 rainfall and evaporative fluxes [ $L T^{-1}$ ]. Surface water velocity at the surface in  $x$  and  $y$  directions,  
 257 ( $v_x$ ) and ( $v_y$ ) respectively, is computed using the following set of equations:

$$258 \quad v_x = \frac{\sqrt{S_{f,x}}}{m} \psi_0^{\frac{2}{3}} \text{ and } v_y = \frac{\sqrt{S_{f,y}}}{m} \psi_0^{\frac{2}{3}} \quad (3)$$

259 Where  $S_{f,x}$  and  $S_{f,y}$  friction slopes along  $x$  and  $y$  respectively and  $m$  is the manning's coefficient.  
 260 ParFlow employs a cell-centered finite difference scheme along with an implicit backward Euler  
 261 scheme and the Newton Krylow linearization method to solve these nonlinear equations. The  
 262 computational grid follows the terrain to mimic the slope of the domain (Maxwell, 2013).

263 ParFlow is coupled to the Community Land Model (CLM, (Dai et al., 2003)) which allows  
 264 for the simulation of important land surface processes such as ET and SWE and the quantification  
 265 of water leaving or entering the surface and subsurface ( $q_s$  and  $q_r$  respectively in the Richards and  
 266 kinematic wave equations). CLM models the thermal processes by closing the energy balance at  
 267 the land surface given by:

$$268 \quad R_n(\theta) = LE(\theta) + H(\theta) + G(\theta) \quad (4)$$

269 Where  $R_n$  is the net radiation at the land surface [ $E/LT$ ] a balance between the shortwave  
 270 and longwave radiation,  $LE$  is the latent heat flux [ $E/LT$ ] which captures the energy required to  
 271 change the phase of water to or from vapor,  $H$  is the sensible heat flux [ $E/LT$ ] and  $G$  is the ground  
 272 heat flux [ $E/LT$ ]. All terms are a function of  $\theta$ , the water content, which is computed by ParFlow.

273 Computing the different components of the energy balance requires meteorological  
 274 forcing, vegetative parameters, and soil moisture. The latter is computed by ParFlow using  
 275 equations 1 and 2. Meteorological forcing includes precipitation, temperature, east to west and  
 276 north to south wind speed, longwave and shortwave solar radiation, air pressure, and relative



277 humidity. Vegetative parameters include maximum and minimum leaf area index, stem area index,  
278 aerodynamic roughness height, optical properties, stomatal physiology, roughness length, and  
279 displacement height. More details about the coupling between ParFlow and CLM as well as the  
280 equations governing the snow dynamics and *ET* can be found in the following papers: Jefferson et  
281 al., (2015); Maxwell & Miller, (2005); Ryken et al., (2020). ParFlow-CLM has been used in many  
282 studies to understand the interactions between groundwater dynamics and lower atmosphere  
283 (Maina et al., 2022; Maina and Siirila-Woodburn, 2020) at different scales from watershed (Foster  
284 and Maxwell, 2019; Maina et al., 2020) to continental scale (Maxwell and Condon, 2016).

### 2.1.2, East River watershed model set-up

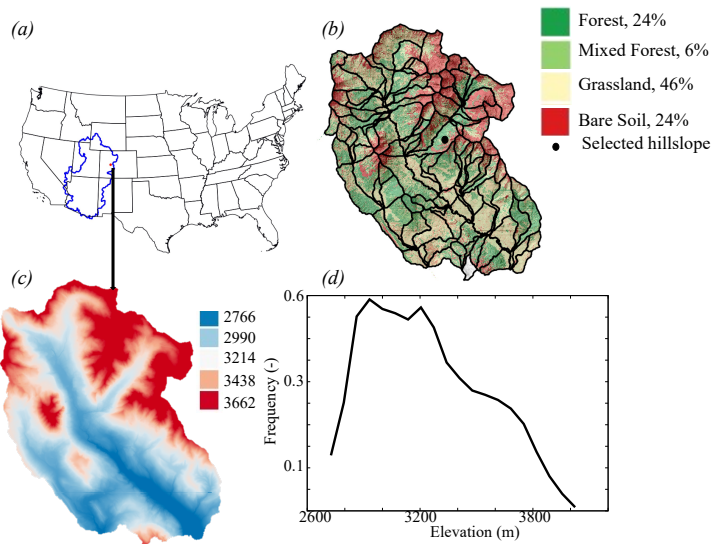
285  
286 The East River watershed (Figure 1), located in the Upper Colorado Basin, is one of the  
287  
288 two major tributaries that form the Gunnison River, which in turn accounts for just under half of  
289 the Colorado River's discharge at the Colorado-Utah border. The total area of this watershed is  
290 approximately 255 km<sup>2</sup> and the elevation varies from approximately ~~2700~~ to ~~3900~~ m. The  
291 watershed is characterized by strong heterogeneities in vegetation, geomorphology, and bedrock  
292 composition (Hubbard et al., 2018). The vegetation includes grasses, conifers, mixed conifers,  
293 aspens, and meadows and lies on a complex geologic terrain, which is comprised of a diverse  
294 collection of Paleozoic and Mesozoic sedimentary and unconsolidated rocks. The watershed is  
295 also characterized by a strong hydroclimate gradient. The average precipitation is 1200 mm/year  
296 while the average temperature is around 0°C. Because of its very low cold winter with temperature  
297 below 0°C, most of the winter precipitation is in the form of snow.  
298

Formatted: Heading 3

Deleted: 2.

Deleted: 3900

Deleted: 2700



302  
 303 Figure 1: (a) location of the East River watershed, (b) land cover (NEON dataset, 2020), (c) LiDAR  
 304 Digital elevation, and (d) elevation distribution within the East River.

305  
 306 ParFlow-CLM used here is based on a previous version of the East River watershed model,  
 307 as described by Foster and Maxwell (2019). 5 layers constitute the model in the vertical direction  
 308 with varying thickness from 0.1 m at the land surface to 21 m at the bottom of the domain. The  
 309 land use and land cover are derived from the high-resolution airborne remote sensing NEON  
 310 campaign (Chadwick, et al., 2020; Falco, et al., 2019; Gouttlen, et al., 2020). From the  
 311 hyperspectral spectrometer and LiDAR readings, 4 major types of land cover are grouped as  
 312 follows: forests (i.e., conifers and aspens), mixed forests, grasses, and bare soil. Parameterization  
 313 of these different land cover types is derived from the IGBP database (IGBP, 2018).

314 The subsurface of the study area is heterogeneous in both vertical and horizontal directions.  
 315 The subsurface of the top 1 m corresponds to three soil layers as defined by the SSURGO database

Deleted: (NEON dataset, 2020).

317 and then corrected based on the land cover and geologic maps to include the outcropping of the  
318 bedrock. Two main types of soil are distinguished within the area: sandy loam and clay loam. The  
319 geology of the subsurface between 1 m and 8 m below the ground was defined with USGS maps,  
320 which were further improved by local knowledge by Pribulick et al., (2016). This subsurface  
321 region is highly heterogeneous with different formations such as crystalline, sedimentary rocks,  
322 unconsolidated rocks, alluvial deposits, and debris flow. The bottom layer of the domain  
323 (extending from 8 m below the ground surface to the bottom of the model) is assumed  
324 homogeneous and represents the fractured bedrock.

325 We simulated the water year (WY) 2015, a relatively average WY in the region based on  
326 average precipitation and temperature patterns. The meteorological forcing of the model has a  
327 resolution of an hour and is derived from two gridded datasets: PRISM and NLDAS. The PRISM  
328 dataset (Daly et al., 2008) is used for precipitation and temperature because of [its](#) accuracy and  
329 high spatial resolution (800m). However, the daily resolution of PRISM impedes its ability to be  
330 used to reproduce diurnal cycles, an important factor when studying land surface processes  
331 requiring hourly forcing. The phase 2 of the North America Land Data Assimilation System  
332 NLDAS-2 forcing (Cosgrove et al., 2003) on the contrary provides hourly changes in precipitation  
333 and temperature yet are only available at coarser, 1/8 degree, resolutions. As such, we employ a  
334 mass-conservative temporal interpolation, which disaggregates the total daily PRISM precipitation  
335 into an hourly time series based on the signal of the NLDAS-2 precipitation and temperature  
336 trends. For the other forcing variables (i.e., shortwave and longwave radiation, wind speed,  
337 atmospheric pressure, and specific humidity), we use NLDAS-2 forcing, (Cosgrove et al., 2003).  
338 [Simulated river stages and SWE were compared to observations in previous studies \(Maina et al.,](#)  
339 [2022; Foster and Maxwell, 2019\). Groundwater measurements are scarce in the watershed and the](#)

Deleted: their

341 majority of the measurements are performed near a station measuring changes in river stages.  
342 Therefore, river stages and groundwater measurements at this point provide similar information.

### 343 **2.2. Hillslopes delineation**

344 As shown in Figure 1b, 127 hillslopes are delineated in the East River watershed based on  
345 the elevation following (Noël et al., 2014) and using Topotoolbox developed by (Schwanghart &  
346 Scherler, 2014). A threshold of flow accumulation was set to match the stream observations at  
347 major tributaries of the East River (Carroll et al., 2018). Because the hillslope delineation could  
348 be sensitive to the threshold of the drainage area, we tested different threshold values to find that  
349 the selected threshold value (810,000 m<sup>2</sup>) represents the scale of hillslope at which the within-  
350 hillslope variability of key properties (such as elevation and aspect) is minimized and hillslope-  
351 averaged properties can account for the majority of watershed-scale variability (Wainwright et al.,  
352 2022).

### 353 **2.3. Hillslopes clustering approaches**

354 We use eight hillslope clustering approaches;

355 1. The  $\Delta P_i$  clustering, proposed in this study, identifies hillslopes with similar groundwater  
356 dynamics. Figure 2 shows the temporal variations of the simulated SWE and WTD at a  
357 selected hillslope (see its location in Figure 1). All hydrologic variables have been  
358 computed at a hillslope scale by computing the arithmetic average of all cells in each  
359 hillslope. In this mountainous watershed, where the largest changes in WTD are mostly a  
360 result of snowmelt, WTD decreases from the beginning of the WY (i.e., October) to the  
361 beginning of snowmelt (i.e., starting from April). As the snow starts to melt and  
362 precipitation starts to fall as rain instead of snow, WTD starts to rise. The shallowest WTD  
363 is June and July when the snow has completely melted and has had time to percolate

Formatted: Heading 2

Moved (insertion) [1]

Formatted: Superscript

Deleted: 1

Deleted: Figure 2 shows the temporal variations of SWE and water table depth at a selected hillslope (see its location in Figure 1) in the watershed. All hydrologic variables have been computed at a hillslope scale by computing the arithmetic average of all cells in each hillslope. In this mountainous watershed, where the largest changes in groundwater are mostly a result of snowmelt, groundwater decreases from the beginning of the WY (i.e. October) to the beginning of snowmelt (i.e. May) period. As the snow starts to melt, groundwater levels start to raise. The peak discharge is mostly observed in June and July when the snow melts over shallow water tables. This period also corresponds to the period of high ET, as both the evaporative demand and the water availability are high. To characterize these groundwater dynamics, we define two variables:  $\Delta P_i$

Formatted: Font: Font color: Black

Formatted: Font: 12 pt, Font color: Black

380 through the unsaturated zone into the groundwater. This period also corresponds to the  
381 period of high ET, because both the evaporative demand and the water availability are high.  
382 The dynamics show two periods characterize the dynamics of the hillslope: from the initial  
383 conditions to the baseflow conditions when the hillslope is losing water, then from  
384 baseflow conditions to the peak of WTD when the hillslope is gaining water. To  
385 characterize these groundwater dynamics, we define two variables:

386 •  $\Delta P_1$  represents the change in WTD between the beginning of the water year and the  
387 deepest WTD during the baseflow conditions. This variable quantifies the amount  
388 of water released by the hillslope during the dry period at the beginning of the water  
389 year. It thus contains information about the amount of water that the hillslope  
390 typically releases/loses, mainly by ET and discharge, given its physical  
391 characteristics and climate dynamics.

392 •  $\Delta P_2$  represents the changes in WTD between the peak flow (i.e., the period with the  
393 shallowest WTD) and the baseflow conditions.  $\Delta P_2$  quantifies the amount of water  
394 gained in the hillslope by recharge, and thus contains information about the  
395 recharge ability of the hillslope given its physical characteristics and climate  
396 dynamics.

397 These two key variables allow us to quantify water release ( $\Delta P_1$ ) and recharge ( $\Delta P_2$ ) within  
398 a hillslope, two key dynamics of the watershed hydrologic function (Sivapalan, 2006; Wagener et  
399 al., 2007; Wainwright et al., 2022). We note that these dynamics are also illustrated by the changes  
400 in measured groundwater levels as depicted in Appendix A.

Deleted: the

Deleted: as

Formatted: Font: 12 pt, Font color: Auto

Formatted: Font: (Default) Times New Roman, Font color: Auto

Formatted: Font: 12 pt, Font color: Auto

Formatted: Font: 12 pt, Font color: Auto, Subscript

Formatted: Font: 12 pt, Font color: Auto

Formatted: Font: (Default) Times New Roman, Font color: Auto

Formatted: List Paragraph, Bulleted + Level: 1 + Aligned at: 0.75" + Indent at: 1", Border: Top: (No border), Bottom: (No border), Left: (No border), Right: (No border), Between : (No border)

Formatted: Font: 12 pt, Font color: Auto

Formatted: Font: 12 pt, Font color: Auto, Subscript

Formatted: Font: 12 pt, Font color: Auto

Formatted: Font: (Default) Times New Roman, Font color: Auto

Formatted: Font: 12 pt, Font color: Auto

Deleted: Two hydrotwo periods, from which depends on the hillslope's

Formatted: Normal, No bullets or numbering

Formatted: Subscript

Formatted: Subscript

Formatted: Indent: Left: 0.75", No bullets or numbering

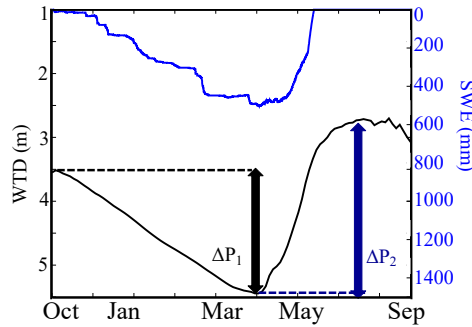
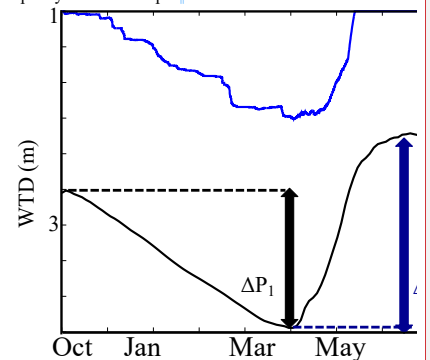


Figure 2: Temporal variations of water table depth (WTD) and SWE at an example hillslope. The location of the hillslope is shown in Figure 1.

2. Elevation: in mountainous watersheds, because the differences in hydroclimate are primarily driven by elevation, hillslopes with similar elevations could potentially have similar land surface processes signatures.
3. Land cover: hillslopes can also be clustered by their dominant land cover. Land cover shapes land surface processes, which in turn affect subsurface dynamics and the water balance at the hillslope scale.
4. TWI: The Topographic Wetness index commonly used to cluster hillslopes is given by:  $\ln\left(\frac{\alpha}{\tan(\beta)}\right)$ . Where  $\alpha$  is the upslope draining area and  $\beta$  the local angle.
5. AI: the AI (ETP/Precipitation, where ETP is the potential evapotranspiration) represents the ratio of the average demand for moisture to the average supply of moisture. We derive the spatial distribution of the AI in the East River from the Global Aridity Index dataset (CGIAR-CSI, 2019).
6. Clustering: we define the hillslope similarity using the clustering of ParFlow-CLM input and output data layers. Clustering was performed in three different ways, using the

**Deleted:**  $\Delta P_1$  represents the changes in groundwater levels between the initial and the minimum groundwater levels during the baseflow conditions. This variable indicates the ability of the hillslope to release water.  
 $\Delta P_2$  quantifies the changes in groundwater levels between the peak flow (i.e. the period with the shallowest water table depth) and the baseflow conditions and hence contains information about the storage and the recharge capacity of the hillslope.



**Deleted:** <#>will

**Formatted:** Font color: Black

**Formatted:** Font color: Black

**Formatted:** Font color: Black

**Formatted:** Font color: Auto

**Formatted:** Font color: Black

**Formatted:** Font color: Black

**Formatted:** Font color: Black

**Formatted:** Font color: Black

**Formatted:** Font color: Black

**Formatted:** Font color: Black

**Formatted:** Font color: Black

**Formatted:** Font color: Black

**Formatted:** Font color: Auto

**Formatted:** Font color: Black

**Formatted:** Font color: Black

**Formatted:** Font color: Auto

**Formatted:** Font color: Black

**Formatted:** Font color: Black

**Formatted:** Font color: Black

457 following data: (1) model input (elevation, percentage of the main land cover type, TWI,  
 458 and AI), referred to hereafter as the “clustering input” (C.I.) method, (2) model output (ET,  
 459 SWE, WTD, and  $\Delta P_1$ ), referred to hereafter as the “clustering output” (C.O.) method, and  
 460 (3) both model input and output data layers, referred to hereafter as the “clustering input-  
 461 output” (C.I.O.) method. We use hierarchical clustering, which is a decision-tree-based  
 462 method that divides data points based on a series of binary splits (Devadoss et al., 2020;  
 463 Kassambara, 2017; Wainwright et al., 2022). We define the linkage (or the distance)  
 464 between any two clusters based on the Euclidian distance and the Ward method that  
 465 computes the variance within each cluster, measuring the distance between each  
 466 observation and the cluster’s mean, and then taking the sum of the distances’ squares.

#### 2.4. Hillslope clustering comparisons

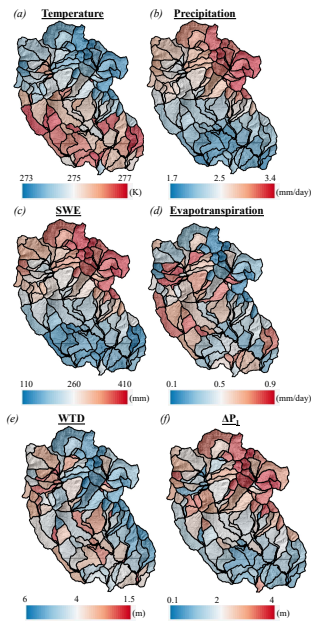
467 To test the ability of the eight selected clustering approaches to identify and categorize  
 468 hillslopes with similar static characteristics and dynamics, we assess each clustering’s ability to  
 469 describe several characteristics of the hillslope: elevation, land cover, hydroclimate (i.e.,  
 470 precipitation), land surface processes (SWE and ET), and subsurface dynamics (WTD values and  
 471 variations). For each clustering, we define three zones. For each variable, zone, and clustering, we  
 472 compute the mean ( $\mu$ ) of the hillslope values and the corresponding coefficient of variation (CV).  
 473 We also calculate the mean of the CV of the different zones for each variable and clustering.

### 3. Results

#### 3.1. Hillslope characteristics

477 Figure 3 shows the spatial distribution of hillslope temperature, precipitation, SWE, ET,  
 478 WTD, and  $\Delta P_1$ .

- Formatted: Font color: Black
- Formatted: Font color: Black, Subscript
- Formatted: Font color: Black
- Formatted: Font color: Black
- Formatted: Heading 2
- Moved (insertion) [2]
- Deleted: classification
- Deleted: s
- Deleted: hydrologic functions
- Deleted: method
- Deleted:
- Deleted: These include a spectrum of datasets varying from those which are widely available (e.g. LULC and elevation) to those which are time-variant (e.g. hydroclimatic data such as temperature and precipitation), and modeled descriptions (e.g. water and energy fluxes).
- Deleted: assification
- Deleted: scheme
- Deleted: ), see Table 1
- Deleted: assification
- Deleted: scheme
- Deleted: This allows us to determine the classification scheme that categorizes zones with the least variability, an important metric that provides a degree of performance for the method’s ability to delineate zones.
- Deleted: and discussions
- Formatted: Heading 2, Outline numbered + Level: 2 + Numbering Style: 1, 2, 3, ... + Start at: 1 + Alignment: Left + Aligned at: 0.75" + Indent at: 1"
- Deleted: functional zonation
- Deleted: ¶
- Moved up [1]: As shown in Figure 1b, 127 hillslopes are delineated in the East River watershed based on the elevation following (Noël et al., 2014) and using Topotoolbox developed by (Schwanghart & Scherler, 2014). A threshold of flow accumulation was set to match the stream observations at major tributaries of the East River (Carroll et al., 2018). Because the hillslope delineation could be sensitive to the threshold of the drainage area, we tested different threshold values to find that the selected threshold value represents the scale of hillslope at which the within-hillslope variability of key properties (such as
- Deleted: classification
- Deleted: some key processes controlling the release... [3]
- Deleted: :
- Deleted: and
- Moved down [3]: As expected, the hillslopes



576  
 577 Figure 3: Spatial distributions of hillslope annual average values of (a) temperature, (b)  
 578 precipitation, (c) snow water equivalent (SWE), (d) evapotranspiration, (e) water table depth  
 579 (WTD) and (e)  $\Delta P_1$

580 As expected, the hillslopes characterized by high SWE have high precipitation and low  
 581 temperatures in contrast to the hillslopes with low SWE. However, ET shows a different pattern,  
 582 because it depends on both water availability and ET demands, which depends on the type of land  
 583 cover. The mid-elevation zone (i.e., zone 2) with a high coverage of forests has high ET. Hillslope  
 584 with high  $\Delta P_1$  have a deep WTD on average, this is because the WTD increases significantly during  
 585 baseflow conditions and reaches very large values as quantified by  $\Delta P_1$ . Hillslopes with high  $\Delta P_1$   
 586 values generally correspond to hillslopes with high precipitation and low temperature and therefore  
 587 high SWE values.

**Deleted:** seasonal changes in groundwater levels

**Moved (insertion) [3]**

**Deleted:** rates

**Formatted:** Font color: Black

**Deleted:** but also the

**Formatted:** Font: 12 pt, Font color: Black

**Deleted:** has more

**Formatted:** Font: 12 pt, Font color: Black

**Formatted:** Font: 12 pt, Font color: Black

**Deleted:** and, therefore,

**Formatted:** Font: 12 pt, Font color: Black

**Formatted:** Font color: Black

**Deleted:** ¶

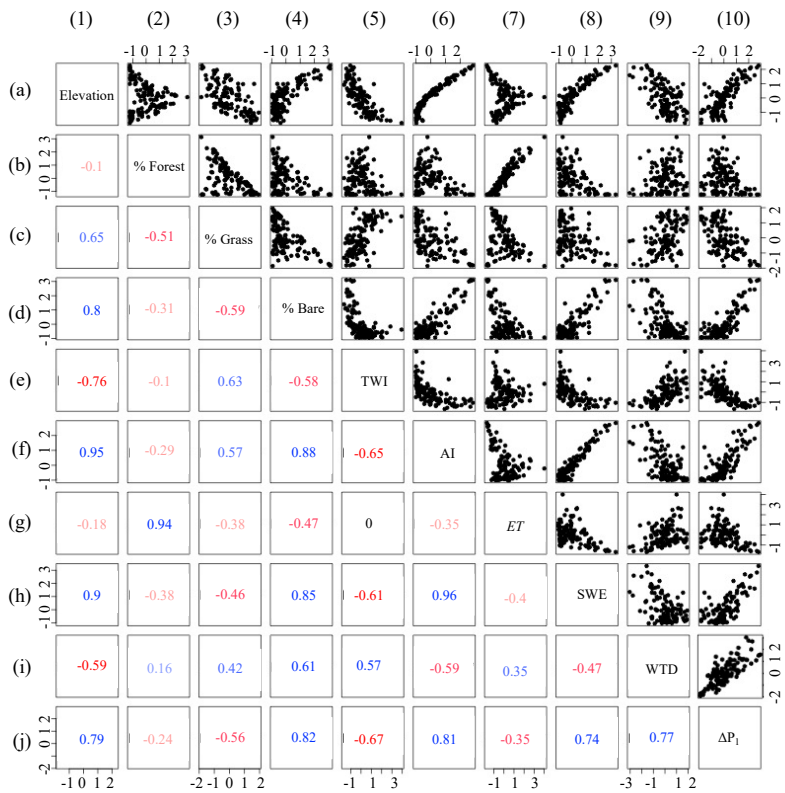
The spatial variability in  $\Delta P_1$  and annual average Water Table Depth (WTD) across different hillslopes are also depicted in Figure 3. These two patterns are different from each other, and they are also different from the ones associated with the land surface processes which eventually control the recharge and release of water (SWE and ET). Nevertheless, the spatial distributions of WTD and  $\Delta P_1$  provide complementary information, with areas with high  $\Delta P_1$  having low WTD because the strong changes in groundwater levels, as

**Deleted:** , lead to a deep WTD

**Deleted:** We also note that the variabilities of these variables within hillslopes are smaller than the ones across hillslopes, which is consistent with Wainwright et al. (2021).



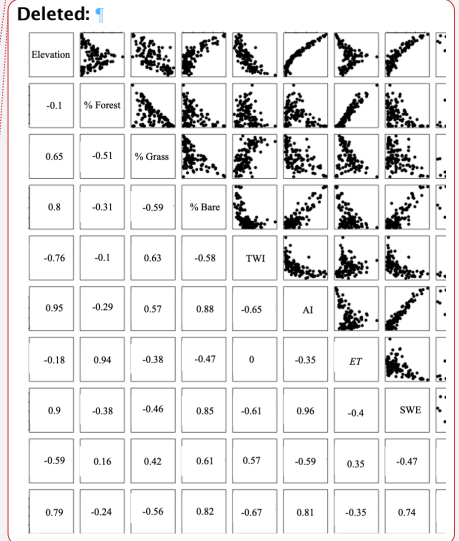
608 To better understand the relationship between  $\Delta P_1$  and the hillslope physical characteristics  
 609 and hydrologic processes, we study the Pearson correlation coefficient between  $\Delta P_1$  and the  
 610 elevation, the percent of the dominant land cover, TWI, AI, ET, SWE, and WTD (Figure 4).



611  
 612 Figure 4: Pearson's correlations between the selected variables for hillslope clustering approaches:  
 613 elevation, percent of the main land cover type (forest, grassland, and bare soil), topographic  
 614 wetness index (TWI), aridity index (AI), evapotranspiration (ET), snow water equivalent (SWE),  
 615 water table depth (WTD), and seasonal changes in groundwater  $\Delta P_1$ . Note that correlation  
 616 coefficients are colored coded based on their values.

**Deleted:** factors controlling the recharge and release of water at a hillslope scale

**Formatted:** Justified, Indent: First line: 0.5"



**Deleted:** similarity classifications

622

623 Results for  $\Delta P_2$  are not shown because  $\Delta P_2$  is strongly correlated to  $\Delta P_1$ . Bare soil, TWI,  
624 AI, SWE, and  $\Delta P_1$  are strongly correlated (we define this as Pearson's correlation coefficient  
625 higher than 0.7) with elevation (Figure 4, column 1, lines d, e, f, h, and j). In particular, elevation  
626 has a dominant control on AI and SWE with a Pearson's correlation coefficient higher than 0.9.  
627 We observe nonlinearity such that TWI increases in the lower elevation and that AI becomes  
628 constant at the lower elevation. High percentage of forests is only found in mid-elevation (Figure  
629 4, 2a) whereas high percentage of grassland is well correlated to low elevations (Figure 4, 3a). ET  
630 is strongly correlated to the percent of forests (Pearson's correlation coefficient is higher than 0.9,  
631 Figure 4 2g).  $\Delta P_1$  has a Pearson's correlation coefficient higher than 0.7 for 6 out of 9 studied  
632 variables (elevation, percent of bare soil, TWI (correlation coefficient equal to 0.67), AI, SWE,  
633 and WTD, Figure 4, line j, columns 1, 4, 5, 6, 8 and 9); it, therefore, indicates that changes  $\Delta P_1$   
634 can reflect the changes of these variables. The two variables with low correlations with  $\Delta P_1$  are ET  
635 and the percent of forests (Figure 4, line j, column 2 and 7). ET is related to groundwater dynamics  
636 in a nonlinear way (Condon et al., 2013; Ferguson & Maxwell, 2010; Rahman et al., 2016). As  
637 shown in these studies, regions with shallow WTDs have the highest ET fluxes and this flux  
638 typically decreases significantly with WTD. When WTD reaches a critical depth, the groundwater  
639 and the atmosphere disconnect and changes in WTD do not impact ET.

640

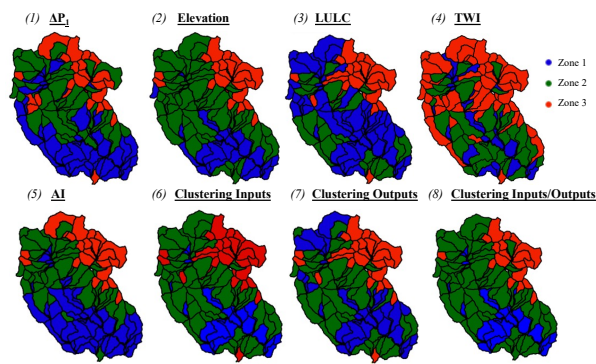
### 641 3.2. Similar hillslopes identification

642 For each clustering, we identify three zones (Figure 5). For the  $\Delta P_1$ , elevation, TWI, and  
643 AI clustering approaches, we define the thresholds of each zone by analyzing the distributions of  
644 the hillslope values of these indices.

**Deleted:** Results for  $\Delta P_2$  are not shown because it is strongly correlated to  $\Delta P_1$  and the two variables provide the same information. TWI, AI, SWE, WTD, and  $\Delta P_1$  are significantly correlated with elevation. In particular, elevation has a dominant control on AI and SWE with a correlation coefficient higher than 0.9. We observe nonlinearity such that TWI increases in the lower elevation and that AI becomes constant at the lower elevation. The percentage of forest cover has a quadratic relationship with elevation. A high correlation between the percent of forests and the elevation is found in the mid-elevation whereas grassland shows a high correlation in low and high elevations. ET is well correlated to the percent of forests, where hillslopes with high ET have a high percent of forests.  $\Delta P_1$  is, in general, well correlated to all these variables; it, therefore, indicates that the selected variable contains valuable information about these variables. Specifically,  $\Delta P_1$  shows a high correlation with SWE, elevation, AI, and WTD with a Pearson correlation coefficient greater than 0.7. Changes in groundwater levels in this mountainous watershed are mostly controlled by the snow dynamics. The two variables with low correlations with  $\Delta P_1$  are the ET (-0.35) and the percent of forests (-0.24). ET is related to groundwater dynamics in a nonlinear way (Condon et al., 2013; Ferguson & Maxwell, 2010; Maina et al., 2022; Rahman et al., 2016). Regions with shallow WTDs have the highest ET fluxes and this flux typically decreases exponentially with the depth, where after a certain threshold a disconnection between the groundwater and the atmosphere occurs, and changes in WTD do not impact ET.

**Formatted:** Heading 2, Outline numbered + Level: 2 + Numbering Style: 1, 2, 3, ... + Start at: 1 + Alignment: Left + Aligned at: 0.75" + Indent at: 1"

680 1.  $\Delta P_1$ : Zone 1 comprises hillslopes whose  $\Delta P_1$  are less than 1.5 m,  $\Delta P_1$  of hillslopes of zone 2 are  
 681 comprised between 1.5 m and 2.5 m, and Zone 3 group all hillslopes with  $\Delta P_1$  greater than 2.5 m.  
 682 1. Elevation: Zone 1 characterizes low elevation areas (average hillslope elevation less than 3000  
 683 m), Zone 2 mid (average hillslope elevation comprises between 3000 m and 3500 m), and Zone 3  
 684 high elevation (hillslope with an average elevation greater than 3500 m).  
 685 3. Land Cover: Zone 1 describes hillslopes that have predominantly grasses as land cover, Zone 2  
 686 for hillslopes with more than 50% of forest, and Zone 3 for hillslopes where bare soil is the  
 687 dominant land cover.  
 688 4. TWI: We define 3 zones with high (TWI>1, Zone 1), mid (TWI comprises between 1 and 0.2  
 689 Zone 2), and low (TWI<0.2, Zone 3) TWI.  
 690 5. AI: Zone 1 comprises hillslopes with AI less than 0.45, Zone 2 describes hillslopes with AI  
 691 between 0.45 and 0.55, and hillslopes of Zone 3 have an AI greater than 0.55.  
 692 6. Clustering: the approaches automatically regroup the similar hillslopes into three zones.



694  
 695 Figure 5: Spatial distribution of hillslope zones derived from the eight selected clustering  
 696 approaches (1)  $\Delta P_1$ , (2) elevation, (3) land cover (LULC), (4) topographic wetness index (TWI),

Formatted: Indent: First line: 0", Border: Top: (No border), Bottom: (No border), Left: (No border), Right: (No border), Between : (No border)

Formatted: Indent: First line: 0.5"

697 (5) aridity index (AI), and clustering with (6) inputs, (7) outputs, and (8) inputs and outputs  
 698 variables.

699 **3.3. Comparisons of the eight selected hillslope clustering approaches**  
 700 Table 1 depicts the mean ( $\mu$ ) and the corresponding coefficient of variation (CV) of  
 701 hillslope values for each variable, zone, and clustering.  
 702

<i>Variable: Elevation</i>				
<b><math>\Delta P_1</math></b>	<b>Elevation</b>	<b>LULC</b>	<b>TWI</b>	
Zone 1: $\mu=3027$ ; CV=0.25	Zone 1: $\mu=2884$ ; CV=0.02	Zone 1: $\mu=3099$ ; CV=0.06	Zone 1: $\mu=2853$ ; CV=0.25	
Zone 2: $\mu=3226$ ; CV=0.06	Zone 2: $\mu=3233$ ; CV=0.06	Zone 2: $\mu=3065$ ; CV=0.16	Zone 2: $\mu=2637$ ; CV=0.41	
Zone 3: $\mu=3593$ ; CV=0.04	Zone 3: $\mu=3641$ ; CV=0.04	Zone 3: $\mu=3595$ ; CV=0.04	Zone 3: $\mu=1999$ ; CV=0.84	
<b>AI</b>	<b>Clustering Input</b>	<b>Clustering Output</b>	<b>Clustering I. O.</b>	
Zone 1: $\mu=2947$ ; CV=0.03	Zone 1: $\mu=3202$ ; CV=0.04	Zone 1: $\mu=3029$ ; CV=0.07	Zone 1: $\mu=3232$ ; CV=0.049	
Zone 2: $\mu=3285$ ; CV=0.03	Zone 2: $\mu=2903$ ; CV=0.03	Zone 2: $\mu=3175$ ; CV=0.04	Zone 2: $\mu=2904$ ; CV=0.034	
Zone 3: $\mu=3625$ ; CV=0.03	Zone 3: $\mu=3592$ ; CV=0.03	Zone 3: $\mu=3605$ ; CV=0.03	Zone 3: $\mu=3658$ ; CV=0.025	
<i>Variable: Precipitation</i>				
<b><math>\Delta P_1</math></b>	<b>Elevation</b>	<b>LULC</b>	<b>TWI</b>	
Zone 1: $\mu=2.24$ ; CV=0.21	Zone 1: $\mu=2.11$ ; CV=0.22	Zone 1: $\mu=2.42$ ; CV=0.22	Zone 1: $\mu=2.38$ ; CV=0.23	
Zone 2: $\mu=2.68$ ; CV=0.18	Zone 2: $\mu=2.77$ ; CV=0.22	Zone 2: $\mu=2.39$ ; CV=0.20	Zone 2: $\mu=2.37$ ; CV=0.22	
Zone 3: $\mu=3.26$ ; CV=0.15	Zone 3: $\mu=3.55$ ; CV=0.09	Zone 3: $\mu=3.26$ ; CV=0.16	Zone 3: $\mu=2.74$ ; CV=0.23	
<b>AI</b>	<b>Clustering Input</b>	<b>Clustering Output</b>	<b>Clustering I. O.</b>	
Zone 1: $\mu=2.10$ ; CV=0.15	Zone 1: $\mu=2.68$ ; CV=0.18	Zone 1: $\mu=2.33$ ; CV=0.22	Zone 1: $\mu=2.73$ ; CV=0.18	
Zone 2: $\mu=2.74$ ; CV=0.17	Zone 2: $\mu=2.06$ ; CV=0.16	Zone 2: $\mu=2.63$ ; CV=0.18	Zone 2: $\mu=2.07$ ; CV=0.17	
Zone 3: $\mu=3.39$ ; CV=0.12	Zone 3: $\mu=3.41$ ; CV=0.11	Zone 3: $\mu=3.43$ ; CV=0.11	Zone 3: $\mu=3.56$ ; CV=0.06	
<i>Variable: Temperature</i>				
<b><math>\Delta P_1</math></b>	<b>Elevation</b>	<b>LULC</b>	<b>TWI</b>	
Zone 1: $\mu=276.5$ ; CV=0.001	Zone 1: $\mu=276.2$ ; CV=0.003	Zone 1: $\mu=276.1$ ; CV=0.002	Zone 1: $\mu=276.3$ ; CV=0.001	
Zone 2: $\mu=275.9$ ; CV=0.002	Zone 2: $\mu=276.0$ ; CV=0.003	Zone 2: $\mu=276.4$ ; CV=0.001	Zone 2: $\mu=276.2$ ; CV=0.002	
Zone 3: $\mu=274.5$ ; CV=0.002	Zone 3: $\mu=274.1$ ; CV=0.002	Zone 3: $\mu=274.4$ ; CV=0.002	Zone 3: $\mu=275.6$ ; CV=0.003	
<b>AI</b>	<b>Clustering Input</b>	<b>Clustering Output</b>	<b>Clustering I. O.</b>	
Zone 1: $\mu=276.6$ ; CV=0.001	Zone 1: $\mu=276.2$ ; CV=0.002	Zone 1: $\mu=276.2$ ; CV=0.002	Zone 1: $\mu=276.1$ ; CV=0.002	
Zone 2: $\mu=275.8$ ; CV=0.002	Zone 2: $\mu=276.5$ ; CV=0.001	Zone 2: $\mu=276.3$ ; CV=0.002	Zone 2: $\mu=276.5$ ; CV=0.001	
Zone 3: $\mu=274.3$ ; CV=0.002	Zone 3: $\mu=274.4$ ; CV=0.003	Zone 3: $\mu=274.3$ ; CV=0.002	Zone 3: $\mu=274.1$ ; CV=0.002	
<i>Variable: SWE</i>				

**Formatted:** Outline numbered + Level: 2 +  
 Numbering Style: 1, 2, 3, ... + Start at: 1 +  
 Alignment: Left + Aligned at: 0.75" + Indent at:  
 1"

**Deleted:** ¶

**Moved up [2]:** To test the ability of the eight selected classifications to identify and categorize hillslopes with similar static characteristics and hydrologic functions, we assess each method's ability to describe several characteristics of the hillslope. These include a spectrum of datasets varying from those which are widely available (e.g. LULC and elevation) to those which are time-variant (e.g. hydroclimatic data such as temperature and precipitation), and modeled descriptions (e.g. water and energy fluxes). For each variable, zone, and classification scheme, we compute the mean ( $\mu$ ) of the hillslope values and the corresponding coefficient of variation (CV), see Table 1. We also calculate the mean of the CV of the different zones for each variable and classification scheme. This allows us to determine the classification scheme that categorizes zones with the least variability, an important metric that provides a degree of performance for the method's ability to delineate zones. ¶

**Deleted:** We examine eight different hillslope classifications using the variables listed below. For each method, three functional zones are delineated (see Figure 5). Except for the clustering approaches, grouping was made based on the manual selection of natural grouping in the probability density function. ¶

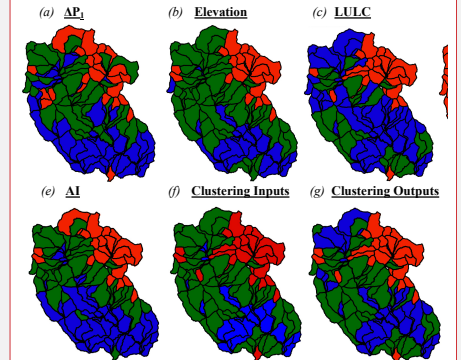


Figure 5: Hillslope zonations based on (a)  $\Delta P_1$ , (b) elevation, (c) land cover (LULC), (d) topographic wetness index (TWI), (e) aridity index (AI), and clustering with (f) inputs, (g) outputs, and (h) inputs and outputs variables. ¶

¶  $\Delta P_1$ : a preliminary analysis of the seasonal changes in groundwater levels allows distinguishing three main hillslope categories with similar  $\Delta P_1$ . Zone 1 comprises hillslopes whose  $\Delta P_1$  are less than 1.5 m,  $\Delta P_1$  of hillslopes of zone 2 are comprised between 1.5 m and 2.5 m, and Zone 3 group all hillslopes with  $\Delta P_1$  greater than 2.5 m. ¶ (... [4])

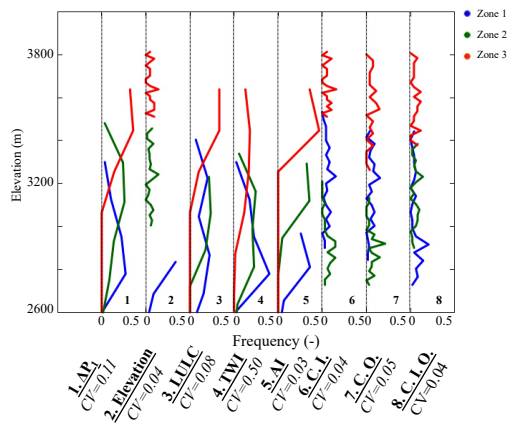
**Deleted:** ¶

<b><u><math>\Delta P_1</math></u></b>	<b><u>Elevation</u></b>	<b><u>LULC</u></b>	<b><u>TWI</u></b>
Zone 1: $\mu=152$ ; CV=0.30 Zone 2: $\mu=204$ ; CV=0.34 Zone 3: $\mu=335$ ; CV=0.31	Zone 1: $\mu=149$ ; CV=0.38 Zone 2: $\mu=201$ ; CV=0.43 Zone 3: $\mu=389$ ; CV=0.26	Zone 1: $\mu=181$ ; CV=0.34 Zone 2: $\mu=151$ ; CV=0.29 Zone 3: $\mu=339$ ; CV=0.29	Zone 1: $\mu=169$ ; CV=0.50 Zone 2: $\mu=165$ ; CV=0.39 Zone 3: $\mu=234$ ; CV=0.46
<b><u>AI</u></b>	<b><u>Clustering Input</u></b>	<b><u>Clustering Output</u></b>	<b><u>Clustering I. O.</u></b>
Zone 1: $\mu=137$ ; CV=0.18 Zone 2: $\mu=206$ ; CV=0.25 Zone 3: $\mu=360$ ; CV=0.24	Zone 1: $\mu=191$ ; CV=0.32 Zone 2: $\mu=145$ ; CV=0.17 Zone 3: $\mu=359$ ; CV=0.25	Zone 1: $\mu=173$ ; CV=0.34 Zone 2: $\mu=179$ ; CV=0.30 Zone 3: $\mu=365$ ; CV=0.23	Zone 1: $\mu=200$ ; CV=0.33 Zone 2: $\mu=146$ ; CV=0.20 Zone 3: $\mu=396$ ; CV=0.18
<b><i>Variable: ET</i></b>			
<b><u><math>\Delta P_1</math></u></b>	<b><u>Elevation</u></b>	<b><u>LULC</u></b>	<b><u>TWI</u></b>
Zone 1: $\mu=0.42$ ; CV=0.47 Zone 2: $\mu=0.41$ ; CV=0.47 Zone 3: $\mu=0.17$ ; CV=0.74	Zone 1: $\mu=0.35$ ; CV=0.75 Zone 2: $\mu=0.48$ ; CV=0.54 Zone 3: $\mu=0.15$ ; CV=0.90	Zone 1: $\mu=0.31$ ; CV=0.36 Zone 2: $\mu=0.61$ ; CV=0.27 Zone 3: $\mu=0.19$ ; CV=0.69	Zone 1: $\mu=0.37$ ; CV=0.58 Zone 2: $\mu=0.41$ ; CV=0.49 Zone 3: $\mu=0.35$ ; CV=0.56
<b><u>AI</u></b>	<b><u>Clustering Input</u></b>	<b><u>Clustering Output</u></b>	<b><u>Clustering I. O.</u></b>
Zone 1: $\mu=0.40$ ; CV=0.46 Zone 2: $\mu=0.45$ ; CV=0.45 Zone 3: $\mu=0.14$ ; CV=0.58	Zone 1: $\mu=0.49$ ; CV=0.37 Zone 2: $\mu=0.25$ ; CV=0.32 Zone 3: $\mu=0.19$ ; CV=0.68	Zone 1: $\mu=0.27$ ; CV=0.29 Zone 2: $\mu=0.55$ ; CV=0.29 Zone 3: $\mu=0.18$ ; CV=0.65	Zone 1: $\mu=0.48$ ; CV=0.38 Zone 2: $\mu=0.25$ ; CV=0.31 Zone 3: $\mu=0.12$ ; CV=0.57
<b><i>Variable: Saturation</i></b>			
<b><u><math>\Delta P_1</math></u></b>	<b><u>Elevation</u></b>	<b><u>LULC</u></b>	<b><u>TWI</u></b>
Zone 1: $\mu=0.77$ ; CV=0.14 Zone 2: $\mu=0.69$ ; CV=0.10 Zone 3: $\mu=0.66$ ; CV=0.11	Zone 1: $\mu=0.75$ ; CV=0.23 Zone 2: $\mu=0.73$ ; CV=0.16 Zone 3: $\mu=0.67$ ; CV=0.13	Zone 1: $\mu=0.75$ ; CV=0.14 Zone 2: $\mu=0.71$ ; CV=0.15 Zone 3: $\mu=0.68$ ; CV=0.09	Zone 1: $\mu=0.81$ ; CV=0.14 Zone 2: $\mu=0.72$ ; CV=0.12 Zone 3: $\mu=0.70$ ; CV=0.13
<b><u>AI</u></b>	<b><u>Clustering Input</u></b>	<b><u>Clustering Output</u></b>	<b><u>Clustering I. O.</u></b>
Zone 1: $\mu=0.75$ ; CV=0.15 Zone 2: $\mu=0.73$ ; CV=0.13 Zone 3: $\mu=0.68$ ; CV=0.11	Zone 1: $\mu=0.72$ ; CV=0.11 Zone 2: $\mu=0.77$ ; CV=0.16 Zone 3: $\mu=0.69$ ; CV=0.09	Zone 1: $\mu=0.76$ ; CV=0.15 Zone 2: $\mu=0.72$ ; CV=0.10 Zone 3: $\mu=0.68$ ; CV=0.09	Zone 1: $\mu=0.72$ ; CV=0.10 Zone 2: $\mu=0.78$ ; CV=0.15 Zone 3: $\mu=0.66$ ; CV=0.08
<b><i>Variable: WTD</i></b>			
<b><u><math>\Delta P_1</math></u></b>	<b><u>Elevation</u></b>	<b><u>LULC</u></b>	<b><u>TWI</u></b>
Zone 1: $\mu=2.9$ ; CV=0.06 Zone 2: $\mu=3.7$ ; CV=0.05 Zone 3: $\mu=4.8$ ; CV=0.07	Zone 1: $\mu=3.4$ ; CV=0.1 Zone 2: $\mu=3.2$ ; CV=0.07 Zone 3: $\mu=4.6$ ; CV=0.08	Zone 1: $\mu=3.0$ ; CV=0.06 Zone 2: $\mu=3.5$ ; CV=0.07 Zone 3: $\mu=4.7$ ; CV=0.07	Zone 1: $\mu=2.4$ ; CV=0.04 Zone 2: $\mu=3.3$ ; CV=0.04 Zone 3: $\mu=4.0$ ; CV=0.1
<b><u>AI</u></b>	<b><u>Clustering Input</u></b>	<b><u>Clustering Output</u></b>	<b><u>Clustering I. O.</u></b>
Zone 1: $\mu=3.1$ ; CV=0.06 Zone 2: $\mu=3.5$ ; CV=0.07 Zone 3: $\mu=4.7$ ; CV=0.08	Zone 1: $\mu=3.2$ ; CV=0.04 Zone 2: $\mu=2.6$ ; CV=0.04 Zone 3: $\mu=4.4$ ; CV=0.06	Zone 1: $\mu=2.8$ ; CV=0.05 Zone 2: $\mu=3.2$ ; CV=0.04 Zone 3: $\mu=4.5$ ; CV=0.05	Zone 1: $\mu=3.3$ ; CV=0.04 Zone 2: $\mu=2.5$ ; CV=0.04 Zone 3: $\mu=4.8$ ; CV=0.05
<b><i>Variable: <math>\Delta P_2</math></i></b>			

$\Delta P_1$	Elevation	LULC	TWI
Zone 1: $\mu=2.9$ ; CV=0.06	Zone 1: $\mu=3.4$ ; CV=0.1	Zone 1: $\mu=3.0$ ; CV=0.06	Zone 1: $\mu=2.4$ ; CV=0.04
Zone 2: $\mu=3.7$ ; CV=0.05	Zone 2: $\mu=3.2$ ; CV=0.07	Zone 2: $\mu=3.5$ ; CV=0.07	Zone 2: $\mu=3.3$ ; CV=0.04
Zone 3: $\mu=4.8$ ; CV=0.07	Zone 3: $\mu=4.6$ ; CV=0.08	Zone 3: $\mu=4.7$ ; CV=0.07	Zone 3: $\mu=4.0$ ; CV=0.1
AI	Clustering Input	Clustering Output	Clustering I. O.
Zone 1: $\mu=3.1$ ; CV=0.06	Zone 1: $\mu=3.2$ ; CV=0.04	Zone 1: $\mu=2.8$ ; CV=0.05	Zone 1: $\mu=3.3$ ; CV=0.04
Zone 2: $\mu=3.5$ ; CV=0.07	Zone 2: $\mu=2.6$ ; CV=0.04	Zone 2: $\mu=3.2$ ; CV=0.04	Zone 2: $\mu=2.5$ ; CV=0.04
Zone 3: $\mu=4.7$ ; CV=0.08	Zone 3: $\mu=4.4$ ; CV=0.06	Zone 3: $\mu=4.5$ ; CV=0.05	Zone 3: $\mu=4.8$ ; CV=0.05

799 Table 1: Mean  $\mu$  and coefficient of variation CV of each variable and hillslope zone derived from  
800 the 8 clustering approaches.

801  
802 **3.1.1. Similarities in hillslope structure**  
803 Elevation plays an important role in the hydroclimate of a region especially in mountainous  
804 watersheds where it controls snow accumulation and controls the downstream hydrology. Figure  
805 6 shows the elevation frequency distributions associated with the 3 zones derived from the 8  
806 clustering approaches.

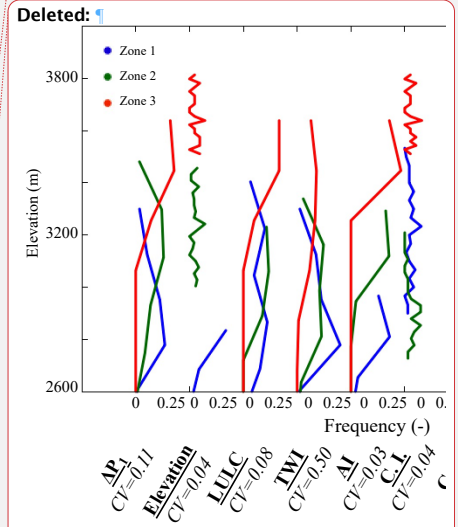


807  
808 Figure 6: Frequency distributions of hillslope elevation. Clustering approaches are based  
809 on  $\Delta P_1$ , elevation, land cover (LULC), topographic wetness index (TWI), aridity index (AI), and

Deleted: classifications  
Formatted: Heading 2, Outline numbered + Level: 3 + Numbering Style: 1, 2, 3, ... + Start at: 1 + Alignment: Left + Aligned at: 1" + Indent at: 1.5"

Deleted: ¶  
Deleted: shaping  
Deleted: given  
Deleted: , the principal driver of  
Deleted: different  
Deleted: classifications

Formatted: Indent: First line: 0.5"



Formatted: Font: 12 pt, Not Italic, Font color: Auto

Formatted: Font: 12 pt, Not Italic, Font color: Auto

Formatted: Font: 12 pt, Not Italic, Font color: Auto

Formatted: Font: 12 pt, Not Italic, Font color: Auto, Subscript

Formatted: Font: 12 pt, Not Italic, Font color: Auto

819 machine-learning approaches (with inputs C.I., outputs C.O., and inputs and outputs C.I.O).  
 820 Hillslope clustering approaches are located across the x-axis. Note that we plotted the distributions  
 821 of the 8 clustering approaches on the same graph, between each dotted line (frequency from 0 to  
 822 0.5) are plotted the frequency distributions of the three zones derived from the clustering.

823  
 824 By classifying the hillslopes using their similarity in  $\Delta P_1$ , we observe that hillslopes with  
 825 low  $\Delta P$  have the lowest elevation while the hillslopes of zone 3 (high  $\Delta P_1$ ) have the highest  
 826 elevation. Unsurprisingly, the second clustering (i.e. elevation) clearly identifies the hillslopes with  
 827 similar elevation. The AI clustering also identifies hillslopes with similar elevation as shown in  
 828 Figures 4 and 6. The TWI clustering performs moderately, where zones 1 and 2 are characterized  
 829 by similar elevation distributions. Hillslopes with lower TWI are mostly located in high elevation  
 830 areas on the contrary to the low elevation hillslopes. In the land cover clustering, most of the  
 831 grassed hillslopes (zone 1) are in low elevation, forests (zone 2) in mid-elevation, and hillslopes  
 832 whose landscape is mainly bare soil (zone 3) are in high elevation areas above the tree line. The  
 833 three clustering approaches using machine learning allow identifying hillslopes with similar  
 834 elevation, their coefficients of variation are of the same order as the elevation clustering.

835 Table 2 describes the average hillslope ratio of land cover type (forests, grassland, and bare  
 836 soil) for each zone and clustering. The land cover clustering indicates that grassland is the  
 837 dominant land cover of zone 1, forests Zone 2, and bare soil zone 3. Only the machine learning  
 838 clustering approaches using outputs lead to a similar conclusion whereas while the other clustering  
 839 approaches capture the characteristics of zone 1 and 3, they do not identify a distinct forested zone  
 840 2. For the  $\Delta P_1$  clustering this could be attributed to the disconnection between groundwater  
 841 dynamics and land surface processes that takes place in certain forested zones. Since clustering

**Formatted:** Font: 12 pt, Not Italic, Font color: Auto

**Formatted:** Font: 12 pt, Not Italic, Font color: Auto

**Deleted:** Distributions of hillslope elevation of the three zones derived from  $\Delta P_1$ , elevation, land cover (LULC), topographic wetness index (TWI), aridity index (AI), and clustering (clustering with inputs C.I., clustering with outputs C.O., and clustering with inputs and outputs C.I.O) hillslope classifications.

**Deleted:** based on

**Deleted:** classification

**Deleted:** scheme

**Deleted:** -based

**Deleted:** distinguishes

**Deleted:** based on their

**Deleted:** , as it is the essence of that classification scheme

**Deleted:** is

**Deleted:** an excellent index for i

**Deleted:** y

**Deleted:** ing

**Deleted:** discussed and

**Deleted:** classification

**Deleted:** -based

**Deleted:** classification

**Deleted:** classifications

**Deleted:**

**Deleted:** distinguishing

**Deleted:** zones

**Deleted:** based classification

**Deleted:** These three classifications lead to similar results indicating that both inputs and outputs yield the same results.

**Deleted:** percentage

**Deleted:** the main

**Deleted:** at the hillslope scale

**Deleted:** classification

**Deleted:** selected

**Deleted:** classification

**Deleted:** s

**Deleted:** lead to similar conclusions, hillslopes associated with zone 1 have mainly grasses, while hillslopes of zone 2 have mostly identical percentage of forest and grasses in the  $\Delta P_1$ , AI, and elevation classifications.

881 based on landscape characteristics and  $\Delta P_1$  do not identify such a distinct zone, it suggests that this  
 882 zone may not be indicative of distinct hydrologic behavior.

Formatted: Subscript

Deleted: LULC classification allows clearly distinguishing zone 1 (grasses) from zone 2 (hillslopes of these zones have more than 70% of forest). For  $\Delta P_1$ , elevation, AI, and LULC classifications, zone 3 is mostly comprised of bare soil, as this zone is mostly located in high elevation areas above the tree line. In the TWI classification, zone 1 is characterized by grasses whereas zone 3's land cover located in high elevation with low TWI is bare soil.

Deleted:

$\Delta P_1$	Forest	Grassland	Bare Soil
Zone 1	0.35	0.55	0.10
Zone 2	0.35	0.43	0.22
Zone 3	0.11	0.27	0.62
CV	0.97	0.56	0.69
Elevation	Forest	Grassland	Bare Soil
Zone 1	0.28	0.56	0.15
Zone 2	0.41	0.42	0.17
Zone 3	0.07	0.26	0.68
CV	1.33	0.76	1.07
Land Cover	Forest	Grassland	Bare Soil
Zone 1	0.23	0.67	0.14
Zone 2	0.72	0.26	0.12
Zone 3	0.12	0.22	0.66
CV	0.67	0.45	0.64
Topographic Wetness Index (TWI)	Forest	Grasslands	Bare Soil
Zone 1	0.24	0.66	0.10
Zone 2	0.35	0.51	0.14
Zone 3	0.32	0.35	0.33
CV	1.47	0.49	0.95
Aridity Index	Forest	Grassland	Bare Soil
Zone 1	0.34	0.57	0.09
Zone 2	0.37	0.41	0.22
Zone 3	0.07	0.32	0.61
CV	0.91	0.56	0.69
Clustering with input layers	Forest	Grassland	Bare Soil
Zone 1	0.44	0.42	0.14
Zone 2	0.11	0.83	0.06
Zone 3	0.12	0.25	0.63
CV	0.83	0.38	0.62



Clustering with output layers	Forest	Grasslands	Bare Soil
Zone 1	0.14	0.77	0.09
Zone 2	0.52	0.34	0.15
Zone 3	0.11	0.25	0.64
CV	0.77	0.38	0.61
Clustering with inputs and outputs	Forest	Grassland	Bare Soil
Zone 1	0.42	0.40	0.18
Zone 2	0.12	0.82	0.06
Zone 3	0.05	0.24	0.70
CV	0.87	0.41	0.65

893 Table 2: Average values of hillslope ratio of forests, grasslands, and bare soils for each zone and

894 clustering.

895 **3.1.2. Similarities in hydroclimate**

896 Figures 7a and b depict the distributions of precipitation and temperature obtained with the

897 eight selected clustering approaches. The AI clustering allows identifying hillslope with similar

898 hydroclimate, because it has low values of coefficients of variation. Zone 1 located in low elevation

899 has low precipitation and high temperatures, contrary to zone 3. Zone 2 is characterized by a

900 hydroclimate that is in between those of Zone 1 and 3. Our ΔP<sub>1</sub> clustering leads to conclusions

901 similar to the machine learning based clustering and AI. These three clustering approaches have

902 the same average CV and are the only methods that allow identifying hillslopes with similar

903 hydroclimate. Although, we note that in the three machine learning based clustering as well as in

904 the ΔP clustering, Zones 1 and 2 have similar hydroclimate, which is not the case in the AI

905 clustering. While the land cover clustering approaches clearly identifies the typical hydroclimate

906 of the hillslopes of zone 3, the two remaining zones have the same hydroclimate. The TWI

907 clustering does not identify hillslopes with similar hydroclimates because it relies on the

908 hydrologic processes driven by the topography. TWI shows that clustering that includes only

Deleted: percentage

Formatted: Indent: First line: 0"

Deleted: classification

Deleted: ¶

Formatted: Heading 2, Outline numbered + Level: 3 + Numbering Style: 1, 2, 3, ... + Start at: 1 + Alignment: Left + Aligned at: 1" + Indent at: 1.5"

Deleted: ¶

Deleted: classifications

Deleted: classifications

Deleted: based on elevation and AI

Deleted: s

Deleted: clearly distinguishing the hydroclimate associated with each zone

Deleted: .

Deleted: rates

Deleted: an intermediate

Deleted: approach based on seasonal variation in groundwater changes

Deleted: based classifications

Deleted: The resulting average CV of these three types of classifications are similar.

Deleted: classifications

Deleted: remain

Deleted: characterizing

Deleted: each zone by its

Deleted: classifications

Deleted: approach

Deleted: based classification

Deleted: classification

Deleted: based on the land cover

Deleted: (bare soil)

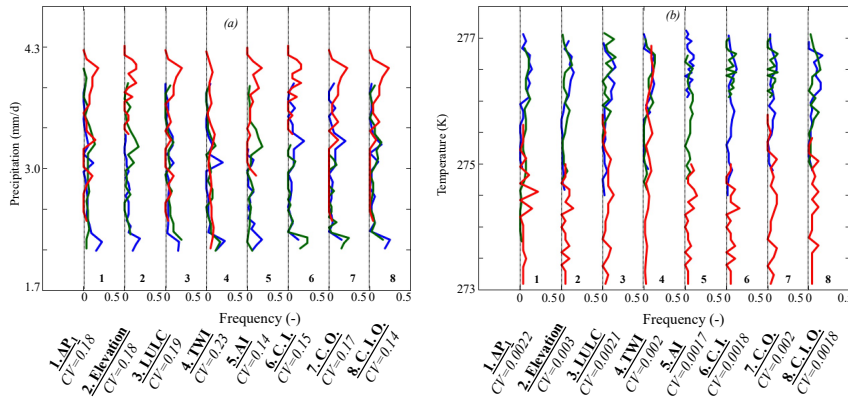
Deleted: classification

Deleted: based on the TWI

Deleted: regroup hillslopes based on their

Deleted: ; again this type of classification mainly describes how a given hillslope release water based on its topographic structure

943 hydroclimate would miss important information on distinct hillslope hydrologic processes that  
 944 strongly affect the response of the hillslope to meteorological forcing.



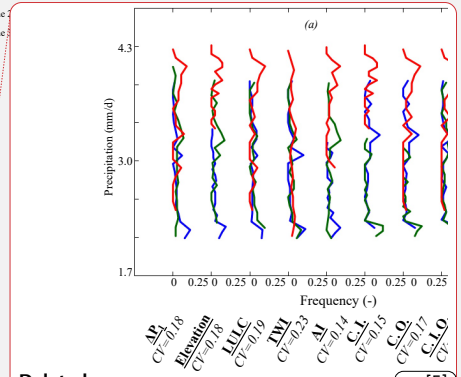
945  
 946 Figure 7: Frequency distributions of hillslope (a) annual average daily rates of precipitation and  
 947 (b) annual average temperature. Clustering approaches are based on  $\Delta P_i$ , elevation, land cover  
 948 (LULC), topographic wetness index (TWI), aridity index (AI), and machine-learning approaches  
 949 (with inputs C.I., outputs C.O., and inputs and outputs C.I.O). Hillslope clustering approaches are  
 950 located across the x-axis. Note that we plotted the distributions of the 8 clustering approaches on  
 951 the same graph, between each dotted line (frequency from 0 to 0.5) are plotted the frequency  
 952 distributions of the three zones derived from the clustering.

### 3.1.3. Similarities in hydrologic processes

954 In this section, we study the ability the selected clustering approaches to identify hillslopes  
 955 with similar hydrologic processes: snow dynamics, evapotranspiration, and WTD values and  
 956 variations.

#### 3.1.3.1. Land surface processes

**Deleted:** Nevertheless, it is important to account for the hydroclimate of hillslopes in a classification.



**Deleted:** ... [5]

**Deleted:** Distributions of hillslope (a) annual average daily rates of precipitation and (b) annual average temperature of the three zones derived from  $\Delta P_i$ , elevation, land cover (LULC), topographic wetness index (TWI), aridity index (AI), and clustering (clustering with inputs C.I., clustering with outputs C.O., and clustering with inputs and outputs C.I.O) hillslope classifications.

**Formatted:** Subscript  
**Formatted:** Heading 2, Outline numbered + Level: 3 + Numbering Style: 1, 2, 3, ... + Start at: 1 + Alignment: Left + Aligned at: 1" + Indent at: 1.5"

**Deleted:** function

**Deleted:** ¶

**Deleted:** Hydrologic processes including land surface and subsurface dynamics are non-linear.

**Deleted:** A hillslope hydrologic function should aim to describe how a hillslope partitions, stores, retains, and releases water. Many hydrologic processes, both at the land surface and in the subsurface, are simultaneously occurring, which typically result in non-linear dynamics.

**Deleted:** show the performance of

**Deleted:** classification

**Deleted:** schemes

**Deleted:** delineate regions exhibiting different surface and subsurface hydrologic behavior. ¶

**Formatted:** Heading 3, Outline numbered + Level: 4 + Numbering Style: 1, 2, 3, ... + Start at: 1 + Alignment: Left + Aligned at: 1.25" + Indent at: 1.75"

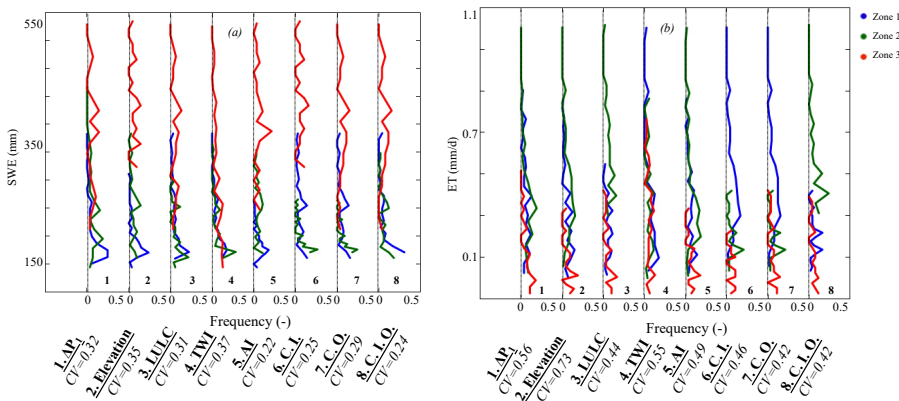
**Deleted:** ¶

984 A robust clustering in mountainous watersheds should identify hillslopes with similar snow  
 985 dynamics. Figure 8a illustrates the SWE frequency distribution associated with each zone and  
 986 clustering. Because SWE dynamics are primarily driven by elevation and the precipitation, the AI  
 987 and machine learning based clustering have the lowest average of the CV followed by the land  
 988 cover and the  $\Delta P_1$  clustering. The land cover spatial distribution contains information about  
 989 elevation especially in high elevation areas where some hillslopes are located above the tree line.  
 990 The  $\Delta P_1$  clustering accounts for SWE dynamics because  $\Delta P_1$  is highly correlated to SWE as  
 991 discussed in section 3.1.

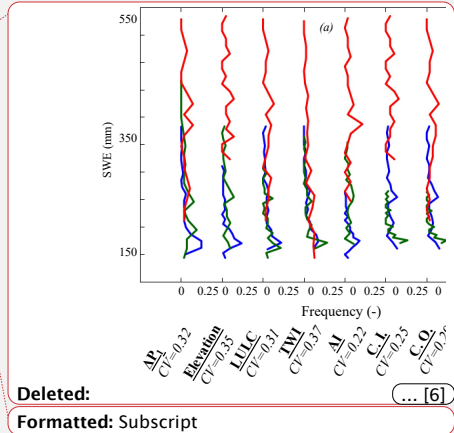
- Deleted:** classification
- Deleted:** of hillslopes
- Deleted:** ntegrate the similarity in
- Deleted:** classification
- Deleted:** classifications
- Deleted:** based on the AI and clustering
- Deleted:** based classification

- Deleted:** approach
- Deleted:**  $\Delta P$  the seasonal changes in groundwater depends on the snowmelt,

**Formatted:** Indent: First line: 0"



992  
 993 **Figure 8:** Frequency distributions of hillslope land surface variables (a) annual average SWE and  
 994 (b) annual average daily rates of ET. Clustering approaches are based on  $\Delta P_1$ , elevation, land cover  
 995 (LULC), topographic wetness index (TWI), aridity index (AI), and machine-learning approaches  
 996 (with inputs C.I., outputs C.O., and inputs and outputs C.I.O). Hillslope clustering approaches are  
 997 located across the x-axis. Note that we plotted the distributions of the 8 clustering approaches on  
 998 the same graph, between each dotted line (frequency from 0 to 0.5) are plotted the frequency  
 999 distributions of the three zones derived from the clustering.



- Deleted:**
- Formatted:** Subscript

1011  
 1012 The spatial distribution of ET is controlled by many factors, including soil moisture, land cover,  
 1013 and subsurface flow. ~~The land cover clustering performs well at identifying hillslopes with similar~~  
 1014 ET ~~because the latter strongly depends on the land cover~~ (Figure 8b). Consistent with the  
 1015 aforementioned results, the other ~~clustering approaches performing well are the machine learning~~  
 1016 ~~based clustering and the AI~~. ~~The TWI and elevation clustering approaches do not separate~~  
 1017 ~~hillslopes by their ET values because they do not account for varying land cover and soil properties~~  
 1018 ~~that influence ET~~. The average CV ~~of the  $\Delta P_1$  clustering is close to those of the land cover and AI~~  
 1019 ~~clustering~~. As stated in many studies (Ferguson & Maxwell, 2010; Maina & Siirila-Woodburn,  
 1020 2020, Maina et al., 2022), subsurface flow affects ET, as such information about subsurface flow  
 1021 contains valuable information about the ET even if the correlation between  $\Delta P_1$  and ET is  
 1022 nonlinear.

**Deleted:** Distributions of hillslope land surface variables (a) annual average SWE and (b) annual average daily rates of ET of the three zones derived from  $\Delta P_1$ , elevation, land cover (LULC), topographic wetness index (TWI), aridity index (AI), and clustering (clustering with inputs C.I., clustering with outputs C.O., and clustering with inputs and outputs C.I.O) hillslope classifications. ¶

**Formatted:** Indent: First line: 0"

**Deleted:** As a result, the...he land cover based...over classification ...lustering performs well at delineating identifying hillslopes with similar ET because the latter strongly depends on the land cover rates... (Figure 8b). Consistent with the aforementioned results, the other classification ...lustering approaches schemes ...erforming well are the machine learning based ones based on clustering and the ...l based classification... ~~The TWI and elevation clustering approaches do not separate hillslopes by their ET values because they do not account for varying land cover and soil properties that influence ET~~. To some extent, the TWI and elevation classifications poorly distinguish hillslopes with similar ET. ...he average CV associated with ...f the  $\Delta P_1$  classification ...lustering is close to that ...hose of the classifications based on ...and cover and AI clustering. As stated in many studies (Ferguson & Maxwell, 2010; Maina & Siirila-Woodburn, 2020, Maina et al., 2022), subsurface flow affects ET, as such information about subsurface flow contains valuable information about the ET even if the correlation between  $\Delta P_1$  and ET is nonlinear. ¶ ... [7]

1023 **3.1.3.2. Similarities in subsurface hydrodynamics**  
 1024 We investigate the ability of the eight selected ~~clustering approaches~~ to identify hillslopes  
 1025 with similar subsurface hydrodynamics. We study the average saturation of the first 10 cm of the  
 1026 soil throughout the WY, the yearly average of ~~WTD~~ and  $\Delta P_2$ . Soil saturation is a key feature in  
 1027 both subsurface and atmospheric dynamics; it controls ET and groundwater recharge. The averages  
 1028 ~~CV of the  $\Delta P_1$ , TWI, AI, land cover, and clustering approaches~~ are very similar (Figure 9a). As  
 1029 the land cover ~~clustering~~ adequately ~~regroup~~ hillslopes with similar ET, it also allows ~~regrouping~~  
 1030 hillslopes with similar soil saturation. ~~Because the TWI describes the characteristics that drive~~  
 1031 ~~flow, it serves as a good indicator of soil saturation like the AI~~. Similar to the results above, the  
 1032 ~~machine learning based clustering perform well~~. The  $\Delta P_1$  ~~clustering~~ has a low average CV due to  
 1033 the strong connection between the changes in ~~WTD~~ and soil saturation. ~~It is only the elevation~~

**Formatted:** Heading 3, Outline numbered + Level: 4 + Numbering Style: 1, 2, 3, ... + Start at: 1 + Alignment: Left + Aligned at: 1.25" + Indent at: 1.75"

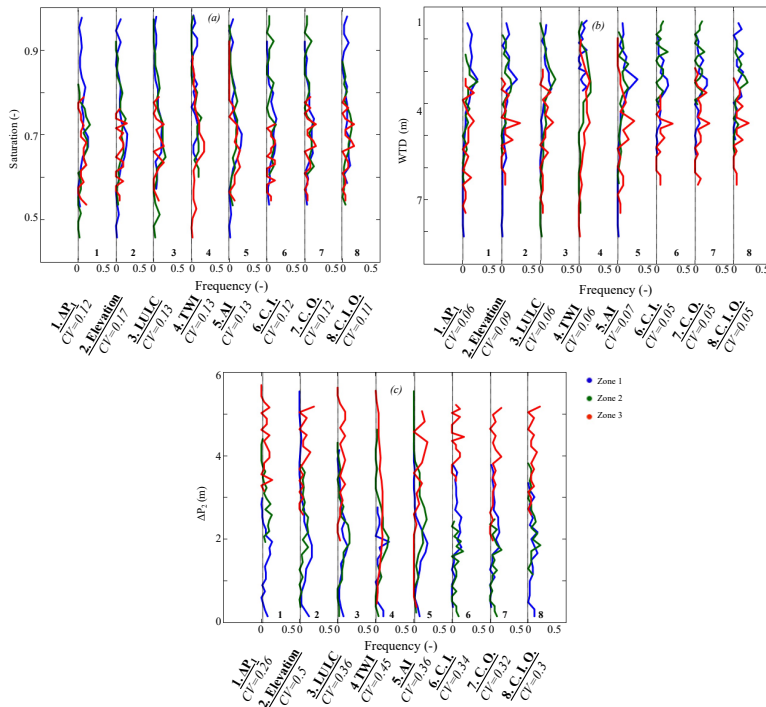
**Deleted:** flow...ydrodynamics ¶ ... [8]

**Deleted:** classifications ...lustering approaches to identify hillslopes with similar subsurface hydrodynamics. We study the average saturation of the first 10 cm of the soil throughout the WY, the yearly average of water table depth...TD,...and the seasonal changes in groundwater levels ... [9]

**Deleted:** Therefore, an appropriate hillslope classification should be able to identify and categorize hillslope with similar soil moisture patterns.

**Deleted:** of the ...V associated with...f the classifications based on ... $P_1$ , TWI, AI, land cover, and clustering approaches are very similar (Figure 9a). As the land cover based classification...lustering adequately regroups hillslopes with similar ET, it also allows regrouping regrouping hillslopes with similar soil saturation. ~~Because the TWI describes the characteristics that drive flow, it serves as a good indicator of soil saturation like the AI~~. Because the TWI approach describes water transfer, it serves transfer, it serves as a good indicator of soil saturation like the AI. ...imilar to the results above, the machine learning based clustering based approaches ...erform well in the classification of hillslopes based on their similarity in saturation... The  $\Delta P_1$  based classification...lustering has one of the... lowest...averages...of ...V due to the stron... [10]

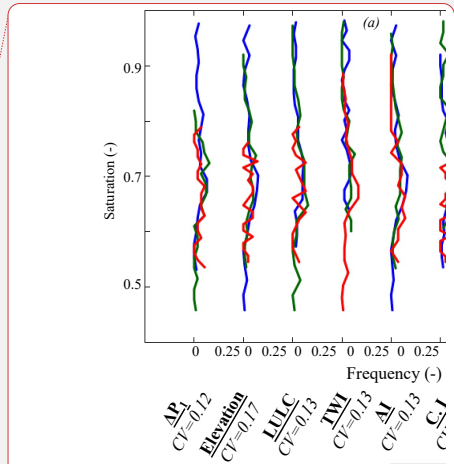
1256 clustering that fails to identify hillslope with similar soil saturation, where the distributions of the  
 1257 three defined zones show overlap.



1258  
 1259 Figure 9: Frequency distributions of hillslope (a) saturation, (b) WTD, and (c)  $\Delta P_2$ . Clustering  
 1260 approaches are based on  $\Delta P_1$ , elevation, land cover (LULC), topographic wetness index (TWI),  
 1261 aridity index (AI), and machine-learning approaches (with inputs C.I., outputs C.O., and inputs  
 1262 and outputs C.I.O). Hillslope clustering approaches are located across the x-axis. Note that we  
 1263 plotted the distributions of the 8 clustering approaches on the same graph, between each dotted  
 1264 line (frequency from 0 to 0.5) are plotted the frequency distributions of the three zones derived  
 1265 from the clustering.

Deleted: on

Formatted: Centered, Indent: First line: 0"



Deleted: ... [11]

Deleted: Distributions of hillslope (a) saturation, (b) WTD, and  $\Delta P_2$  of the three zones derived from  $\Delta P_1$ , elevation, land cover (LULC), topographic wetness index (TWI), aridity index (AI), and clustering (clustering with inputs C.I., clustering with outputs C.O., and clustering with inputs and outputs C.I.O) hillslope classifications.

Formatted: Subscript

Deleted:

1275  
 1276 WTD is an important variable for determining groundwater storage. Here, we rely on the  
 1277 average WTD throughout the year. As expected, the  $\Delta P_1$  clustering identifies hillslopes with  
 1278 similar WTD (Figure 9b). Zone 1 located in low elevation has the shallowest WTD and the lowest  
 1279  $\Delta P_1$ , contrary to zone 3. Zone 2 exhibits a behavior that is in between those of Zone 1 and 3. The  
 1280 TWI and land cover clustering approaches also are good for identifying hillslope with similar  
 1281 WTD. Hillslopes with low TWI (Zone 3) have the deepest WTD, contrary to the hillslopes of Zone  
 1282 1. The TWI identifies hillslopes with similar WTD because of the high relief of the watershed that  
 1283 drive its hydrology (Fan et al., 2019). The land cover clustering indicates that most of the forest  
 1284 (Zone 2) and bare soil (Zone 3) hillslopes have deep WTD whereas grasses (Zone 1) hillslopes  
 1285 have the shallowest WTD. The elevation clustering doesn't accurately identify hillslopes with  
 1286 similar WTD, and its average CV remains higher than the 4 other clustering approaches. The AI,  
 1287 like the elevation, isn't a good variable for identifying hillslopes with similar WTD. All their three  
 1288 zones overlap in terms of WTD. Results from the machine learning based clustering are similar to  
 1289 the  $\Delta P_1$  clustering with a CV of the same order, yet there isn't a clear distinction between Zone 1  
 1290 and 2 in these machine learning based clustering approaches.

**Deleted:** Groundwater storage is mostly quantified in terms of WTD. ...TD is an important variable for determining groundwater storage at a hillslope scale... Here, we quantify ...ely on the average WTD throughout the year. As expected, the  $\Delta P_1$  based classification...ustering groups identifies hillslopes with similar WTD (Figure 9b). Zone 1 located in low elevation has the shallowest WTD and the lowest  $\Delta P_1$ , contrary to zone 3. Zone 2 exhibits an intermediary... behavior that is in between those of Zone 1 and 3. The TWI and land cover classification...ustering approaches schemes ...so are good methods ...or hillslope with similar changes in ...TD. Hillslopes with low TWI (Zone 3) have the deepest WTD, contrary to the hillslopes of Zone 1. The TWI classification ...dentifies hillslopes with similar WTD because of the high relief of the watershed that drive the...ts hydrology (Fan et al., 2019). (cite Haurko's paper). ...he land cover based classification...ustering indicates that most of the forest (Zone 2) and bare soil (Zone 3) hillslopes have deep WTD whereas grasses (Zone 1) hillslopes have the shallowest WTD. The elevation-based...classification ...ustering scheme ...oesn't accurately regroup ...dentify hillslopes with similar WTD, and its average CV remains higher than the 4 other classification ...ustering approacheschemes... The AI method... like the elevation method... isn't a good variable for identifying hillslopes with similar WTD. In fact, a...ll their three zones overlap in terms of WTD even if their AIs are distinct... Results from the machine learning based clustering approach ...re similar to the  $\Delta P_1$  based classification...ustering with a CV of the same order, yet there isn't a clear distinction between Zone 1 and 2 in these approaches ... [12]

1291 Figure 9c illustrates the distributions of the  $\Delta P_2$  for each clustering approach and zone.  $\Delta P_1$   
 1292 clusters hillslopes with similar  $\Delta P_2$  as expected. Another suitable clustering approach for hillslopes  
 1293 with similar  $\Delta P_2$  is the land cover. Zone 3 characterizing bare soil hillslopes has the highest  $\Delta P_2$ ,  
 1294 unlike zones 1 and 2. The AI clustering shows that the majority of zone 3 hillslopes have high  $\Delta P_2$   
 1295 whereas zone 2 hillslopes have low  $\Delta P_2$ , followed by zone 1 hillslopes. In terms of  $\Delta P_2$  similarity,  
 1296 the elevation clustering outperforms the TWI. The machine learning based clustering approaches  
 1297 are good for identifying hillslopes with similar  $\Delta P_2$  especially the clustering using inputs variables

**Deleted:** seasonal changes in groundwater levels ... or each classification ...ustering approach and zone. The ... $P_1$  classification based on  $\Delta P_1$  groups ...usters hillslopes with similar  $\Delta P_2$  as expected. Another suitable approach clustering approach to ...or group ...illslopes with similar  $\Delta P_2$  is the land cover classification... Zone 3 characterizing bare soil hillslopes has the highest  $\Delta P_2$ , unlike zones 1 and 2. The AI classification ...ustering shows that the majority of zone 3 hillslopes have high  $\Delta P_2$  whereas zone 2 hillslopes have low  $\Delta P_2$ , followed by zone 1 hillslopes. In terms of  $\Delta P_2$  similarity, the elevation-based... classification...ustering outperforms the TWI. The machine learning based clustering approaches ...pproaches area ...re good way of...or identifying with ...illslopes with similar  $\Delta P_2$  especially the clustering approach based...sing on ... [13]

1421 (CI). The two other machine learning based clustering approaches (outputs and inputs and outputs)  
1422 do not distinguish zone 1 from zone 2.

1423 **4. Discussions**  
1424 In this section, we discuss the advantages of the proposed  $\Delta P_1$  clustering compared to the  
1425 other clustering approaches and its ability to capture dry and wet hydrologic conditions.

1426 **4.1. Advantages of the  $\Delta P_1$  clustering**  
1427 Depending on the purpose of the identification of similar hillslopes, the appropriate  
1428 clustering may change. Nonetheless, it is important for any clustering approach to identify  
1429 hillslopes with similar hydrologic processes. As demonstrated here, the advantage of using  $\Delta P_1$  to  
1430 identify similar hillslopes is that many hydrologic processes are embedded in  $\Delta P_1$ . Our  
1431 comparisons have shown that by using a  $\Delta P_1$  clustering, one is able to identify hillslopes with not  
1432 only similar subsurface hydrodynamics but also similar land surface processes. Because these  
1433 processes are intimately linked to the physical characteristics of the hillslope, its hydroclimate, and  
1434 its land cover, the  $\Delta P_1$  clustering also allows for the identification of hillslopes with the  
1435 aforementioned characteristics similar.

1436 We, however, highlight that other clustering approaches may outperform the  $\Delta P_1$  when  
1437 looking at a single characteristic. For instance, our results show that the elevation and AI clustering  
1438 approaches may be excellent at identifying hillslopes with similar hydroclimates and snow  
1439 dynamics. The land cover clustering allows for better identification of hillslopes with similar land  
1440 surface processes such as ET and soil saturation. Lastly, the TWI clustering allows the  
1441 identification of hillslopes with similar groundwater dynamics and soil saturation values as it  
1442 describes the topographic flow. In terms of overall performance, our results show that for the study  
1443 site considered here, the machine learning based clustering approaches are also a very good at  
1444 identifying similar hillslopes.

- Deleted: clustering approaches
- Deleted: ¶
- Deleted: classification
- Deleted: compared to other existing classifications and its ability to capture dry and wet hydrologic
- Deleted:
- Formatted: Heading 2, Outline numbered + Level: 2 + Numbering Style: 1, 2, 3, ... + Start at: 1 + Alignment: Left + Aligned at: 0.75" + Indent at: 1"
- Deleted: a similarity
- Deleted: index
- Deleted: based  $\Delta P_1$
- Deleted: classification
- Deleted: scheme
- Deleted: classification
- Deleted: functions
- Deleted: the seasonal changes in groundwater
- Deleted: classification
- Deleted: scheme to identify hillslopes of similar nature
- Deleted: group
- Deleted: regions
- Deleted: based on
- Deleted: dynamics
- Deleted: structure, the static
- Deleted: , and the physical properties
- Deleted: approach
- Deleted: topographic structures, land cover, and hydroclimates...
- Deleted: For these reasons,  $\Delta P_1$  could be considered as an integrated variable for hillslope similarity that does (... [14])
- Deleted: classifications
- Deleted: a single process or
- Deleted: classifications
- Deleted: approaches to group
- Deleted: based classification
- Deleted: classification
- Deleted: scheme
- Deleted: grouping
- Deleted: water transfer
- Deleted: the
- Deleted: approach is
- Deleted: approach for hillslope classification.

1488 Wainwright et al., (2022) use an unsupervised clustering method and remote sensing data  
1489 layers which include elevation, SWE, radiation, resistivity, and Normalized Difference Vegetation  
1490 Index NDVI to define 7 clusters in the East River watershed. While their clustering method has  
1491 more zones (7) than ours (3), it leads to similar conclusions as our study where zones 1 and 2 are  
1492 characterized by low elevation, high TWI, and low SWE values contrary to zones 5 and 6.

1493 Other hillslope clustering approaches based on hydrologic processes relied on the Peclet  
1494 number (Berne et al., 2005; S. W. Lyon & Troch, 2007; Steve W. Lyon & Troch, 2010) which  
1495 describes the subsurface hydrological response and is derived from an analytical solution of the  
1496 subsurface flow (e.g. the Boussinesq storage equation (Steve W. Lyon & Troch, 2010)). However,  
1497 while the three-dimensional Richards equation has the advantage of better representing the  
1498 subsurface flow it cannot be solved analytically, hence these indices cannot be applied to integrated  
1499 hydrologic models. Our approach has demonstrated that the  $\Delta P$  helps quantify the subsurface  
1500 hydrologic responses without using these indices and therefore overcomes the limitation of the use  
1501 of attributes such as the Peclet number on integrated hydrologic models to categorize hillslopes.

#### 1503 4.2. Similarities in hydrologic responses to wet and dry conditions.

1504 According to McDonnell & Woods, (2004) and Wagener et al., (2007), any classification  
1505 should be able to predict the dynamics of the hillslopes. We test the ability of the  $\Delta P_1$  clustering to  
1506 predict the dynamics of the hillslopes in wet and dry conditions. A possible limitation of a  
1507 clustering based on a hydrologic process is that the latter may be linked to the conditions of the  
1508 selected year. Hydrologic responses are by essence nonlinear and may strongly change from year  
1509 to year. In addition, compared to the intrinsic characteristics of the hillslope (elevation,  
1510 topographic index, and land cover), which are only variable if long periods of time are considered;  
1511 the scale at which hydrologic processes change is much shorter. Therefore, a clustering based on

Deleted: ¶

Formatted: Heading 2, Outline numbered + Level: 2 + Numbering Style: 1, 2, 3, ... + Start at: 1 + Alignment: Left + Aligned at: 0.75" + Indent at: 1"

Deleted: based classification

Deleted: classification

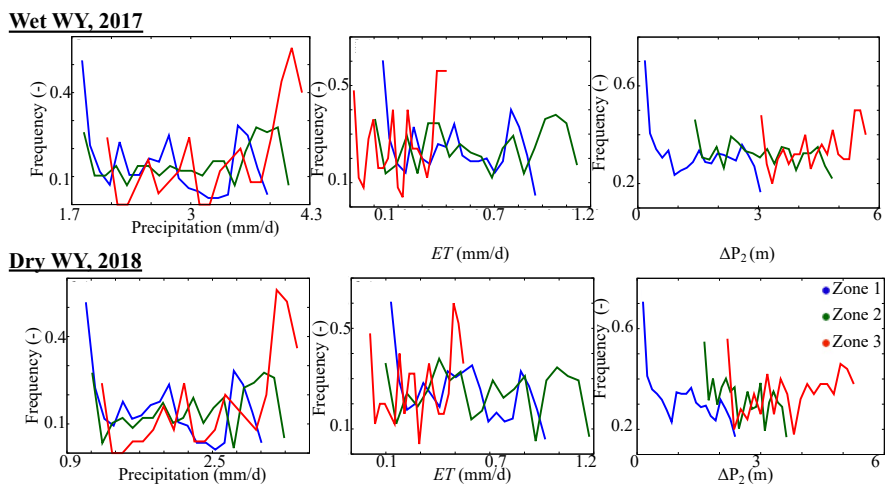
Deleted: classification

Deleted: scheme



1517 a hydrologic process may be time-dependent. We previously quantified  $\Delta P_1$  using an average WY.  
 1518 In this section, we compare the response of each zone to dry and wet conditions. We extend our  
 1519 simulation from the WY 2015 to include the WYs 2016, 2017, and 2018, then we analyze WYs  
 1520 2017 and 2018. This 4-year simulation covers a relatively wet (2017) and dry (2018) WY. The  
 1521 annual average precipitation in 2017 was ~15% higher than the annual average precipitation in  
 1522 2015. After this wet WY, the watershed is characterized by a dry climate in 2018, with average  
 1523 precipitation almost 50% below the normal conditions. Figure 10 shows the distributions of  
 1524 hillslope annual average values of precipitation and ET, and the hillslope  $\Delta P_2$  associated with the  
 1525 defined  $\Delta P_1$  zones and for both the wet WY 2017 and the dry WY 2018. We have selected the key  
 1526 variables describing the hydroclimate (Precipitation), land surface processes (ET), and subsurface  
 1527 hydrodynamics ( $\Delta P_2$ ).

Deleted: process-based approach  
 Deleted: the seasonal changes in groundwater in



1528

1529 Figure 10: Frequency distributions of hillslope annual average daily rates of precipitation and  
 1530 evapotranspiration (ET), and the hillslope seasonal changes in groundwater levels ( $\Delta P_2$ ) in 2017  
 1531 (wet WY) and 2018 (dry WY) of the three zones derived from the WY 2015  $\Delta P_1$

Deleted: D

1535

1536 At first glance, for both dry and wet years and selected processes, all zones remain distinct.

1537 Zone 1 with hillslopes with low  $\Delta P_1$  located in low elevation remains with low precipitation, high

1538 ET, through both wet and dry years. Zone 3 describing hillslopes with high  $\Delta P_1$  has the highest

1539 precipitation in the area during both the wet and dry years. Hillslopes of zone 2, located in mid-

1540 elevation, have most of their hydrologic dynamics in between those of zone 1 and 3 except their

1541 ET, which is the highest in the area due to the presence of forest. Our results show that although

1542 we defined hillslopes clustering based on a hydrologic process during an average WY, our

1543 clustering approach can predict the similarity of the dynamics of these hillslopes in wet and dry

1544 conditions. The  $\Delta P_1$  clustering is, therefore, robust in predicting similarity in hydrologic responses

1545 under both wet and dry conditions.

1546

### 1547 5. Summary and conclusions

1548 In this study, we use seasonal changes in groundwater levels, termed  $\Delta P_1$ , to identify and

1549 categorize similar hillslopes.  $\Delta P_1$  is an important variable controlled by many hydrologic processes

1550 including land surface processes and hydroclimatic. We defined three zones based on their

1551 similarity in  $\Delta P_1$ . For a test case site in the East River watershed, zone 1 characterizes hillslopes

1552 with low  $\Delta P_1$ ; these hillslopes are mostly located in low elevation areas, their main land cover is

1553 grassland, and their ET is high because their WTDs are shallow. Zone 3, on the opposite of zone

1554 1 is located in high elevation areas and has high  $\Delta P_1$ ; the hydroclimate leads to high snow

1555 accumulation and low ET. Hillslopes of zone 3 are mostly bare soil. Zone 2 is in-between these

1556 two zones, most of the hillslopes of this zone are covered by forests.

1557 We tested the performance of the proposed  $\Delta P_1$  clustering by comparing it with other

1558 existing clustering approaches based on elevation, land cover, aridity index, a topographic wetting

Deleted: regrouping

Deleted: seasonal changes in groundwater

Deleted: , and low seasonal changes in groundwater

Deleted: seasonal changes in groundwater

Deleted: classification

Deleted: classification

Deleted: based classification

Deleted: approach

Formatted: Heading 1, Outline numbered + Level: 1 + Numbering Style: 1, 2, 3, ... + Start at: 3 + Alignment: Left + Aligned at: 0.5" + Indent at: 0.75"

Deleted: ¶

Deleted: the

Deleted: , termed

Deleted: (see definition in Figure 2),

Deleted: The seasonal change in groundwater

Deleted: and unique

Deleted: as

Deleted: effects propagate to affect this variableit

Deleted: Our results show that the  $\Delta P_1$  classification allows transcending the uniqueness of place inherent in traditional classifications.

Deleted: ability

Deleted: based classification

Deleted: to identify and group hillslopes with similar static characteristics and hydrologic processes

Deleted: approaches

1583 index, and three clustering approaches based on machine learning which uses multiple data layers,  
1584 including model inputs and outputs. Our results show that the  $\Delta P_1$  clustering is robust, as it  
1585 reasonably identifies and categorizes hillslopes with similar elevation, land cover, hydroclimate  
1586 characteristics, land surface processes (ET and SWE), and subsurface hydrodynamics (WTD, soil  
1587 moisture, and  $\Delta P_1$ ). In general, the other clustering approaches are good in identifying similarity  
1588 in a single characteristic, related to the variable determining the clustering. Our work also  
1589 demonstrates that a clustering using machine learning, either based on top-down (inputs) or  
1590 bottom-up (outputs) performs well. Nevertheless, these clustering approaches like the  $\Delta P_1$  require  
1591 multiple datasets, each one with its own associated uncertainty. We further demonstrate the  
1592 robustness of the proposed  $\Delta P_1$  clustering by testing its ability to predict hillslope responses to wet  
1593 and dry hydrologic conditions. The  $\Delta P_1$  values are derived from a model and could be a limitation  
1594 for sites where simulated outputs are unavailable, or the spatio-temporal resolution of groundwater  
1595 observations are limited. In addition, one of the main limitations of the proposed clustering is that  
1596 due to the disconnection between land surface processes and structures and the subsurface  
1597 dynamics in some regions, this clustering approach cannot be used in these conditions.

1598 Future studies could aim to identify similar hillslopes using  $\Delta P_1$  and sophisticated machine  
1599 learning approaches or optimization procedures. Our results are limited to one catchment, which  
1600 has snow-dominated hydrology. Future studies could expand the comparison shown here to other  
1601 watersheds, to include additional clustering approaches, and for different hydroclimate and  
1602 durations of time (for example, sub-annual or multi-annual clustering).

### 1603 **Data availability**

1604 Data supporting the findings of this study are freely available on ESS-DIVE:

1605 <https://ess-dive.lbl.gov>

Deleted: s

Deleted: based classification

Deleted: water table depths

Deleted: seasonal changes in water table fluctuations

Deleted: approaches

Deleted: , a characteristic that is

Deleted: selected

Deleted: which

Deleted: es

Deleted: classification

Deleted: scheme

Deleted: approach

Deleted: approaches

Deleted: based classification

Deleted: based classification

Deleted: used in this demonstration

Deleted: We also highlight that

Deleted: classification

Deleted: it may not be useful in these regions.

Deleted: This study demonstrates the need for an integrated variable such as groundwater changes to identify and group similar hillslopes.

Deleted: define functional zones

Deleted: based on their seasonal changes in groundwater using

Deleted: classifications

Deleted: classifications

Deleted: ¶

1634            **Author contribution**

1635            The authors contribute equally to this work.

1636            **Competing interests**

1637            The authors declare that they have no conflict of interest.

1638

1639            **Acknowledgements**

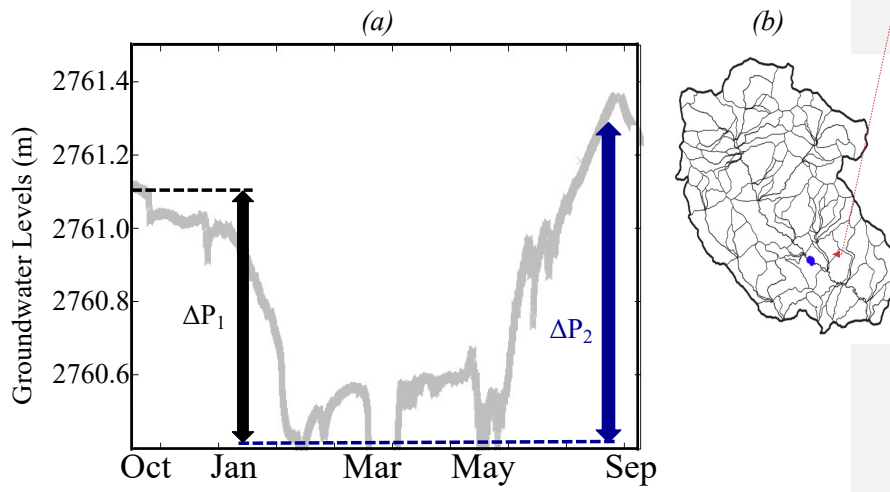
1640            This material is based on work supported as part of the Watershed Function Scientific Focus Area

1641            funded by the U.S. Department of Energy, Office of Science, Office of Biological and

1642            Environmental Research under Award no. DE-AC02-05CH11231.

1643

**Appendix A**



**Formatted: Font: Bold**

**Formatted: Justified**

1644

1645

**Figure A1: (a) Measured groundwater levels in WY2016 at a station located in blue in (b)**

**Formatted: Font: Not Bold**

**Formatted: Centered**

**Formatted: Font: Not Bold**

1646                   **References**

1647

- 1648   Andréassian, V., Lerat, J., Le Moine, N., & Perrin, C. (2012). Neighbors: Nature's own  
1649       hydrological models. *Journal of Hydrology*, 414–415, 49–58.  
1650       <https://doi.org/10.1016/j.jhydrol.2011.10.007>
- 1651   Aryal, S. K., O'Loughlin, E. M., & Mein, R. G. (2002). A similarity approach to predict landscape  
1652       saturation in catchments. *Water Resources Research*, 38(10), 26-1-26–16.  
1653       <https://doi.org/10.1029/2001WR000864>
- 1654   Berghuijs, W. R., Sivapalan, M., Woods, R. A., & Savenije, H. H. G. (2014). Patterns of similarity  
1655       of seasonal water balances: A window into streamflow variability over a range of time  
1656       scales. *Water Resources Research*, 50(7), 5638–5661.  
1657       <https://doi.org/10.1002/2014WR015692>
- 1658   Berne, A., Uijlenhoet, R., & Troch, P. A. (2005). Similarity analysis of subsurface flow response  
1659       of hillslopes with complex geometry. *Water Resources Research*, 41(9).  
1660       <https://doi.org/10.1029/2004WR003629>
- 1661   Beven, K. J. (2000). Uniqueness of place and process representations in hydrological modelling.  
1662       *Hydrology and Earth System Sciences*, 4(2), 203–213. [https://doi.org/10.5194/hess-4-203-](https://doi.org/10.5194/hess-4-203-2000)  
1663       2000
- 1664   BEVEN, K. J., & KIRKBY, M. J. (1979). A physically based, variable contributing area model of  
1665       basin hydrology / Un modèle à base physique de zone d'appel variable de l'hydrologie du  
1666       bassin versant. *Hydrological Sciences Bulletin*, 24(1), 43–69.  
1667       <https://doi.org/10.1080/02626667909491834>
- 1668   Bormann, H. (2010). Towards a hydrologically motivated soil texture classification. *Geoderma*,  
1669       157(3), 142–153. <https://doi.org/10.1016/j.geoderma.2010.04.005>

1670 Bosch, J. M., & Hewlett, J. D. (1982). A review of catchment experiments to determine the effect  
 1671 of vegetation changes on water yield and evapotranspiration. *Journal of Hydrology*, 55(1),  
 1672 3–23. [https://doi.org/10.1016/0022-1694\(82\)90117-2](https://doi.org/10.1016/0022-1694(82)90117-2)

1673 Brown, A. E., Zhang, L., McMahon, T. A., Western, A. W., & Vertessy, R. A. (2005). A review  
 1674 of paired catchment studies for determining changes in water yield resulting from  
 1675 alterations in vegetation. *Journal of Hydrology*, 310(1), 28–61.  
 1676 <https://doi.org/10.1016/j.jhydrol.2004.12.010>

1677 Brunner, P., & Simmons, C. T. (2012). HydroGeoSphere: A Fully Integrated, Physically Based  
 1678 Hydrological Model. *Groundwater*, 50(2), 170–176. [https://doi.org/10.1111/j.1745-](https://doi.org/10.1111/j.1745-6584.2011.00882.x)  
 1679 [6584.2011.00882.x](https://doi.org/10.1111/j.1745-6584.2011.00882.x)

1680 Carrillo, G., Troch, P. A., Sivapalan, M., Wagener, T., Harman, C., & Sawicz, K. (2011).  
 1681 Catchment classification: hydrological analysis of catchment behavior through process-  
 1682 based modeling along a climate gradient. *Hydrology and Earth System Sciences*, 15(11),  
 1683 3411–3430. <https://doi.org/10.5194/hess-15-3411-2011>

1684 Carroll, R. W. H., Bearup, L. A., Brown, W., Dong, W., Bill, M., & Williams, K. H. (2018).  
 1685 Factors controlling seasonal groundwater and solute flux from snow-dominated basins.  
 1686 *Hydrological Processes*, 32(14), 2187–2202. <https://doi.org/10.1002/hyp.13151>

1687 CGIAR-CSI. (2019, January 24). Global Aridity Index and Potential Evapotranspiration Climate  
 1688 Database v2. Retrieved August 22, 2020, from  
 1689 <https://cgiarcsi.community/2019/01/24/global-aridity-index-and-potential->  
 1690 [evapotranspiration-climate-database-v2/](https://cgiarcsi.community/2019/01/24/global-aridity-index-and-potential-)

1691 [Chadwick, K. D., Brodrick, P. G., Grant, K., Goulden, T., Henderson, A., Falco, N., Wainwright,](#)  
 1692 [H., Williams, K. H., Bill, M., Breckheimer, I., Brodie, E. L., Steltzer, H., Rick Williams,](#)

Formatted: Font: (Default) Times New Roman, 12 pt, Font color: Black

Formatted: Font: (Default) Times New Roman, 12 pt, Font color: Black, Pattern: Clear

Formatted: Font: (Default) Times New Roman, 12 pt, Font color: Black

Formatted: Font: (Default) Times New Roman, 12 pt, Font color: Black, Pattern: Clear

Formatted: Font: (Default) Times New Roman, 12 pt, Font color: Black

Formatted: Font: (Default) Times New Roman, 12 pt, Font color: Black, Pattern: Clear

Formatted: Font: (Default) Times New Roman, 12 pt, Font color: Black

Formatted: Font: (Default) Times New Roman, 12 pt, Font color: Black, Pattern: Clear

Formatted: Font: (Default) Times New Roman, 12 pt, Font color: Black

Formatted: Font: (Default) Times New Roman, 12 pt, Font color: Black, Pattern: Clear

Formatted: Font: (Default) Times New Roman, 12 pt, Font color: Black

Formatted: Font: (Default) Times New Roman, 12 pt, Font color: Black, Pattern: Clear

Formatted: Font: (Default) Times New Roman, 12 pt, Font color: Black

Formatted: Font: (Default) Times New Roman, 12 pt, Font color: Black, Pattern: Clear

Formatted: Font: (Default) Times New Roman, 12 pt, Font color: Black

Formatted: Font: (Default) Times New Roman, 12 pt, Font color: Black, Pattern: Clear

Formatted: Font: (Default) Times New Roman, 12 pt, Font color: Black

Formatted: Font: (Default) Times New Roman, 12 pt, Font color: Black, Pattern: Clear

Formatted: Font: (Default) Times New Roman, 12 pt, Font color: Black

Formatted: Font: (Default) Times New Roman, 12 pt, Font color: Black, Pattern: Clear

Formatted: Font: (Default) Times New Roman, 12 pt, Font color: Black

Formatted: Font: (Default) Times New Roman, 12 pt, Font color: Black, Pattern: Clear

Formatted: Font: (Default) Times New Roman, 12 pt, Font color: Black

Formatted: Font: (Default) Times New Roman, 12 pt, Font color: Black

Formatted: Font: (Default) Times New Roman, 12 pt, Font color: Black





1715 Devadoss, J., Falco, N., Dafflon, B., Wu, Y., Franklin, M., Hermes, A., et al. (2020). Remote  
1716 Sensing-Informed Zonation for Understanding Snow, Plant and Soil Moisture Dynamics  
1717 within a Mountain Ecosystem. *Remote Sensing*, 12(17), 2733.  
1718 <https://doi.org/10.3390/rs12172733>

1719 Fan, Y., Clark, M., Lawrence, D. M., Swenson, S., Band, L. E., Brantley, S. L., et al. (2019).  
1720 Hillslope Hydrology in Global Change Research and Earth System Modeling. *Water*  
1721 *Resources Research*, 55(2), 1737–1772. <https://doi.org/10.1029/2018WR023903>

1722 [Fan, Y., Clark, M., Lawrence, D. M., Swenson, S., Band, L. E., Brantley, S. L., Brooks, P. D.,  
1723 Dietrich, W. E., Flores, A., Grant, G., Kirchner, J. W., Mackay, D. S., McDonnell, J. J.,  
1724 Milly, P. C. D., Sullivan, P. L., Tague, C., Ajami, H., Chaney, N., Hartmann, A.,  
1725 Hazenberg, P., McNamara, J., Pelletier, J., Perket, J., Rouholahnejad-Freund, E., Wagener,  
1726 T., Zeng, X., Beighley, E., Buzan, J., Huang, M., Livneh, B., Mohanty, B. P., Nijssen, B.,  
1727 Safeeq, M., Shen, C., van Verseveld, W., Volk, J., and Yamazaki, D. \(2019\), Hillslope  
1728 hydrology in global change research and Earth system modeling, \*Water Resour. Res.\*, 55,  
1729 1737–1772. <https://doi.org/10.1029/2018WR023903>.](#)

1730 [Falco N ; Balde A ; Breckheimer I ; Brodie E ; G. Brodrick P ; Chadwick K D ; Chen J ; Dafflon  
1731 B ; Henderson A ; Lamb J ; Maher K ; Kueppers L ; Steltzer H ; Wainwright H ; Williams  
1732 K ; S. Hubbard S \(2020\): Plant species distribution within the Upper Colorado River Basin  
1733 estimated by using hyperspectral and LiDAR airborne data. Watershed Function SFA,  
1734 ESS-DIVE repository. Dataset. doi:10.15485/1602034, accessed via \[https://data.ess-  
dive.lbl.gov/datasets/doi:10.15485/1602034\]\(https://data.ess-<br/>1735 dive.lbl.gov/datasets/doi:10.15485/1602034\), on 2022-03-29](#)

Formatted: Font: (Default) Times New Roman, 12 pt, Font color: Black, Pattern: Clear

Formatted: Font: (Default) Times New Roman, 12 pt, Font color: Black, Pattern: Clear

Formatted: Font color: Black

Formatted: Font: (Default) Times New Roman, 12 pt, Font color: Black, Pattern: Clear

Formatted: Font: (Default) Times New Roman, 12 pt, Font color: Black

Formatted: Default Paragraph Font, Font: (Default) Times New Roman, 12 pt, Font color: Black

Formatted: Font: (Default) Times New Roman, 12 pt, Font color: Black

Formatted: Default Paragraph Font, Font: (Default) Times New Roman, 12 pt, Font color: Black

Formatted: Font: (Default) Times New Roman, 12 pt, Font color: Black

1736 Ferguson, I. M., & Maxwell, R. M. (2010). Role of groundwater in watershed response and land  
 1737 surface feedbacks under climate change. *Water Resources Research*, 46(10).  
 1738 <https://doi.org/10.1029/2009WR008616>

1739 Freeze, R. A., & Harlan, R. L. (1969). Blueprint for a physically-based, digitally-simulated  
 1740 hydrologic response model. *Journal of Hydrology*, 9(3), 237–258.  
 1741 [https://doi.org/10.1016/0022-1694\(69\)90020-1](https://doi.org/10.1016/0022-1694(69)90020-1)

1742 Foster, L.M., Williams, K.H., Maxwell, R.M., 2020. Resolution matters when modeling climate  
 1743 change in headwaters of the Colorado River. *Environ. Res. Lett.*  
 1744 <https://doi.org/10.1088/1748-9326/aba77f>

1745 van Genuchten, M. Th. (1980). A Closed-form Equation for Predicting the Hydraulic Conductivity  
 1746 of Unsaturated Soils1. *Soil Science Society of America Journal*, 44(5), 892.  
 1747 <https://doi.org/10.2136/sssaj1980.03615995004400050002x>

1748 Grabs, T., Seibert, J., Bishop, K., & Laudon, H. (2009). Modeling spatial patterns of saturated  
 1749 areas: A comparison of the topographic wetness index and a dynamic distributed model.  
 1750 *Journal of Hydrology*, 373(1), 15–23. <https://doi.org/10.1016/j.jhydrol.2009.03.031>

1751 Goulden T ; Hass B ; Brodie E ; Chadwick K D ; Falco N ; Maher K ; Wainwright H ; Williams  
 1752 K (2020): NEON AOP Survey of Upper East River CO Watersheds: LAZ Files, LiDAR  
 1753 Surface Elevation, Terrain Elevation, and Canopy Height Rasters. Watershed Function  
 1754 SFA, ESS-DIVE repository. Dataset. doi:10.15485/1617203, accessed via https://data.ess-  
 1755 dive.lbl.gov/datasets/doi:10.15485/1617203, on 2022-03-29

1756 Harman, C., & Sivapalan, M. (2009). A similarity framework to assess controls on shallow  
 1757 subsurface flow dynamics in hillslopes. *Water Resources Research*, 45(1).  
 1758 <https://doi.org/10.1029/2008WR007067>

Formatted: Font: (Default) Times New Roman, 12 pt, Font color: Black

Formatted: Default Paragraph Font, Font: (Default) Times New Roman, 12 pt, Font color: Black

Formatted: Font: (Default) Times New Roman, 12 pt, Font color: Black

Formatted: Default Paragraph Font, Font: (Default) Times New Roman, 12 pt, Font color: Black

Formatted: Font: (Default) Times New Roman, 12 pt, Font color: Black

1759 Hjerdt, K. N., McDonnell, J. J., Seibert, J., & Rodhe, A. (2004). A new topographic index to  
1760 quantify downslope controls on local drainage. *Water Resources Research*, 40(5).  
1761 <https://doi.org/10.1029/2004WR003130>

1762 Hubbard, S. S., Williams, K. H., Agarwal, D., Banfield, J., Beller, H., Bouskill, N., et al. (2018).  
1763 The East River, Colorado, Watershed: A Mountainous Community Testbed for Improving  
1764 Predictive Understanding of Multiscale Hydrological–Biogeochemical Dynamics. *Vadose*  
1765 *Zone Journal*, 17(1), 180061. <https://doi.org/10.2136/vzj2018.03.0061>

1766 IGBP. (2018). Global plant database published - IGBP [text]. Retrieved October 17, 2018, from  
1767 [http://www.igbp.net/news/news/news/globalplantdatabasepublished.5.1b8ae20512db692f](http://www.igbp.net/news/news/news/globalplantdatabasepublished.5.1b8ae20512db692f2a6800014762.html)  
1768 [2a6800014762.html](http://www.igbp.net/news/news/news/globalplantdatabasepublished.5.1b8ae20512db692f2a6800014762.html)

1769 Jefferson, J. L., Gilbert, J. M., Constantine, P. G., & Maxwell, R. M. (2015). Active subspaces for  
1770 sensitivity analysis and dimension reduction of an integrated hydrologic model. *Computers*  
1771 *& Geosciences*, 83, 127–138. <https://doi.org/10.1016/j.cageo.2015.07.001>

1772 Kassambara, A. (2017). *Practical guide to cluster analysis in R: Unsupervised machine learning*  
1773 (Vol. 1). Sthda.

1774 Loritz, R., Kleidon, A., Jackisch, C., Westhoff, M., Ehret, U., Gupta, H., & Zehe, E. (2019). A  
1775 topographic index explaining hydrological similarity by accounting for the joint controls  
1776 of runoff formation. *Hydrology and Earth System Sciences*, 23(9), 3807–3821.  
1777 <https://doi.org/10.5194/hess-23-3807-2019>

1778 Lyon, S. W., & Troch, P. A. (2007). Hillslope subsurface flow similarity: Real-world tests of the  
1779 hillslope Péclet number. *Water Resources Research*, 43(7).  
1780 <https://doi.org/10.1029/2006WR005323>

1781 Lyon, Steve W., & Troch, P. A. (2010). Development and application of a catchment similarity  
1782 index for subsurface flow. *Water Resources Research*, 46(3).  
1783 <https://doi.org/10.1029/2009WR008500>

1784 Maina, F. Z., & Siirila-Woodburn, E. R. (2020). The Role of Subsurface Flow on  
1785 Evapotranspiration: A Global Sensitivity Analysis. *Water Resources Research*, 56(7),  
1786 e2019WR026612. <https://doi.org/10.1029/2019WR026612>

1787 ~~Maina, Fadji Z., Siirila-Woodburn, E. R., & Dennedy-Frank, P. J. (2022) Assessing the impacts of~~  
1788 ~~hydrodynamic parameter uncertainties on simulated evapotranspiration in a mountainous~~  
1789 ~~watershed. *Journal of Hydrology* 608. <https://doi.org/10.1016/j.jhydrol.2022.127620>,~~

1790 Maxwell, R. M. (2013). A terrain-following grid transform and preconditioner for parallel, large-  
1791 scale, integrated hydrologic modeling. *Advances in Water Resources*, 53, 109–117.  
1792 <https://doi.org/10.1016/j.advwatres.2012.10.001>

1793 Maxwell, R. M., & Miller, N. L. (2005). Development of a Coupled Land Surface and  
1794 Groundwater Model. *Journal of Hydrometeorology*, 6(3), 233–247.  
1795 <https://doi.org/10.1175/JHM422.1>

1796 McDonnell, J. J., & Woods, R. (2004). On the need for catchment classification. *Journal of*  
1797 *Hydrology*, 299, 2–3. <https://doi.org/10.1016/j.jhydrol.2004.09.003>

1798 ~~Noël, P., Rousseau, A. N., Paniconi, C., & Nadeau, D. F. (2014). Algorithm for Delineating and~~  
1799 ~~Extracting Hillslopes and Hillslope Width Functions from Gridded Elevation Data. *Journal*~~  
1800 ~~of *Hydrologic Engineering*, 19(2), 366–374. [Formatted: Border: Top: \(No border\), Bottom: \(No border\), Left: \(No border\), Right: \(No border\), Between : \(No border\)](https://doi.org/10.1061/(ASCE)HE.1943-</a></del><br/>1801 <del>5584.0000783</del></p></div><div data-bbox=)~~

Formatted: Font color: Text 1

Deleted: NEON dataset. (2020). Land Cover and Processes | NSF NEON | Open Data to Understand our Ecosystems. Retrieved May 7, 2020, from <https://www.neonscience.org/data/data-themes/land-cover-processes>

1807 Oudin, L., Kay, A., Andréassian, V., & Perrin, C. (2010). Are seemingly physically similar  
1808 catchments truly hydrologically similar? *Water Resources Research*, 46(11).  
1809 <https://doi.org/10.1029/2009WR008887>

1810 Pribulick, C. E., Foster, L. M., Bearup, L. A., Navarre-Sitchler, A. K., Williams, K. H., Carroll, R.  
1811 W. H., & Maxwell, R. M. (2016). Contrasting the hydrologic response due to land cover  
1812 and climate change in a mountain headwaters system. *Ecohydrology*, 9(8), 1431–1438.  
1813 <https://doi.org/10.1002/eco.1779>

1814 Rahman, M., Sulis, M., & Kollet, S. J. (2016). Evaluating the dual-boundary forcing concept in  
1815 subsurface–land surface interactions of the hydrological cycle. *Hydrological Processes*,  
1816 30(10), 1563–1573. <https://doi.org/10.1002/hyp.10702>

1817 Richards, L. A. (1931). Capillary conduction of liquids through porous medium. *Journal of*  
1818 *Applied Physics*, 1(5), 318–333. <https://doi.org/10.1063/1.1745010>

1819 Ryken, A., Bearup, L. A., Jefferson, J. L., Constantine, P., & Maxwell, R. M. (2020). Sensitivity  
1820 and model reduction of simulated snow processes: Contrasting observational and  
1821 parameter uncertainty to improve prediction. *Advances in Water Resources*, 135, 103473.  
1822 <https://doi.org/10.1016/j.advwatres.2019.103473>

1823 Sawicz, K., Wagener, T., Sivapalan, M., Troch, P. A., & Carrillo, G. (2011). Catchment  
1824 classification: empirical analysis of hydrologic similarity based on catchment function in  
1825 the eastern USA. *Hydrology and Earth System Sciences*, 15(9), 2895–2911.  
1826 <https://doi.org/10.5194/hess-15-2895-2011>

1827 Schwanghart, W., & Scherler, D. (2014). Short Communication: TopoToolbox 2 – MATLAB-  
1828 based software for topographic analysis and modeling in Earth surface sciences. *Earth*  
1829 *Surface Dynamics*, 2(1), 1–7. <https://doi.org/10.5194/esurf-2-1-2014>

1830 SIVAPALAN, M., TAKEUCHI, K., FRANKS, S. W., GUPTA, V. K., KARAMBIRI, H.,  
1831 LAKSHMI, V., et al. (2003). IAHS Decade on Predictions in Ungauged Basins (PUB),  
1832 2003–2012: Shaping an exciting future for the hydrological sciences. *Hydrological*  
1833 *Sciences Journal*, 48(6), 857–880. <https://doi.org/10.1623/hysj.48.6.857.51421>  
1834 Wagener, T., Sivapalan, M., Troch, P., & Woods, R. (2007). Catchment Classification and  
1835 Hydrologic Similarity. *Geography Compass*, 1(4), 901–931.  
1836 <https://doi.org/10.1111/j.1749-8198.2007.00039.x>  
1837 Wainwright, H. M., Uhlemann, S., Franklin, M., Falco, N., Bouskill, N. J., Newcomer, M.,  
1838 Dafflon, B., Woodburn, E., Minsley, B. J., Williams, K. H., and Hubbard, S. S. (2022).  
1839 Watershed zonation approach for tractably quantifying above-and-belowground watershed  
1840 heterogeneity and functions, *Hydrol. Earth Syst. Sci.*, <https://doi.org/10.5194/hess-2021->  
1841 228.  
1842

Deleted: 1

Deleted: Discuss. [preprint]

Deleted: , in review

Page 14: [1] Deleted Maina, Fadji Zaouna (GSFC-6170)[UNIVERSITY OF MARYLAND  
BALTIMORE CO] 2/18/22 9:11:00 AM

Page 14: [2] Formatted Maina, Fadji Zaouna (GSFC-6170)[UNIVERSITY OF MARYLAND  
BALTIMORE CO] 2/18/22 9:18:00 AM

List Paragraph, Numbered + Level: 1 + Numbering Style: 1, 2, 3, ... + Start at: 1 + Alignment:  
Left + Aligned at: 0.25" + Indent at: 0.5", Border: Top: (No border), Bottom: (No border), Left:  
(No border), Right: (No border), Between : (No border)

Page 15: [3] Deleted Maina, Fadji Zaouna (GSFC-6170)[UNIVERSITY OF MARYLAND  
BALTIMORE CO] 2/18/22 9:24:00 AM

Page 20: [4] Deleted Maina, Fadji Zaouna (GSFC-6170)[UNIVERSITY OF MARYLAND  
BALTIMORE CO] 2/17/22 2:20:00 PM

Page 26: [5] Deleted Maina, Fadji Zaouna (GSFC-6170)[UNIVERSITY OF MARYLAND  
BALTIMORE CO] 2/17/22 6:43:00 PM

Page 27: [6] Deleted Maina, Fadji Zaouna (GSFC-6170)[UNIVERSITY OF MARYLAND  
BALTIMORE CO] 2/17/22 6:44:00 PM

Page 28: [7] Deleted Maina, Fadji Zaouna (GSFC-6170)[UNIVERSITY OF MARYLAND  
BALTIMORE CO] 2/18/22 10:06:00 AM

Page 28: [7] Deleted Maina, Fadji Zaouna (GSFC-6170)[UNIVERSITY OF MARYLAND  
BALTIMORE CO] 2/18/22 10:06:00 AM

Page 28: [7] Deleted Maina, Fadji Zaouna (GSFC-6170)[UNIVERSITY OF MARYLAND  
BALTIMORE CO] 2/18/22 10:06:00 AM

Page 28: [7] Deleted Maina, Fadji Zaouna (GSFC-6170)[UNIVERSITY OF MARYLAND  
BALTIMORE CO] 2/18/22 10:06:00 AM

Page 28: [7] Deleted Maina, Fadji Zaouna (GSFC-6170)[UNIVERSITY OF MARYLAND  
BALTIMORE CO] 2/18/22 10:06:00 AM

Page 28: [7] Deleted Maina, Fadji Zaouna (GSFC-6170)[UNIVERSITY OF MARYLAND  
BALTIMORE CO] 2/18/22 10:06:00 AM

Page 28: [7] Deleted Maina, Fadji Zaouna (GSFC-6170)[UNIVERSITY OF MARYLAND  
BALTIMORE CO] 2/18/22 10:06:00 AM

Page 28: [7] Deleted Maina, Fadji Zaouna (GSFC-6170)[UNIVERSITY OF MARYLAND  
BALTIMORE CO] 2/18/22 10:06:00 AM

Page 28: [7] Deleted Maina, Fadji Zaouna (GSFC-6170)[UNIVERSITY OF MARYLAND  
BALTIMORE CO] 2/18/22 10:06:00 AM

Page 28: [7] Deleted Maina, Fadji Zaouna (GSFC-6170)[UNIVERSITY OF MARYLAND  
BALTIMORE CO] 2/18/22 10:06:00 AM



Page 28: [7] Deleted Maina, Fadji Zaouna (GSFC-6170)[UNIVERSITY OF MARYLAND BALTIMORE CO] 2/18/22 10:06:00 AM

Page 28: [7] Deleted Maina, Fadji Zaouna (GSFC-6170)[UNIVERSITY OF MARYLAND BALTIMORE CO] 2/18/22 10:06:00 AM

Page 28: [7] Deleted Maina, Fadji Zaouna (GSFC-6170)[UNIVERSITY OF MARYLAND BALTIMORE CO] 2/18/22 10:06:00 AM

Page 28: [7] Deleted Maina, Fadji Zaouna (GSFC-6170)[UNIVERSITY OF MARYLAND BALTIMORE CO] 2/18/22 10:06:00 AM

Page 28: [7] Deleted Maina, Fadji Zaouna (GSFC-6170)[UNIVERSITY OF MARYLAND BALTIMORE CO] 2/18/22 10:06:00 AM

Page 28: [7] Deleted Maina, Fadji Zaouna (GSFC-6170)[UNIVERSITY OF MARYLAND BALTIMORE CO] 2/18/22 10:06:00 AM

Page 28: [8] Deleted Maina, Fadji Zaouna (GSFC-6170)[UNIVERSITY OF MARYLAND BALTIMORE CO] 2/22/22 8:47:00 AM

Page 28: [8] Deleted Maina, Fadji Zaouna (GSFC-6170)[UNIVERSITY OF MARYLAND  
BALTIMORE CO] 2/22/22 8:47:00 AM

3.1.1.2

Page 28: [9] Deleted Maina, Fadji Zaouna (GSFC-6170)[UNIVERSITY OF MARYLAND  
BALTIMORE CO] 4/6/22 1:12:00 PM

Page 28: [9] Deleted Maina, Fadji Zaouna (GSFC-6170)[UNIVERSITY OF MARYLAND  
BALTIMORE CO] 4/6/22 1:12:00 PM

Page 28: [9] Deleted Maina, Fadji Zaouna (GSFC-6170)[UNIVERSITY OF MARYLAND  
BALTIMORE CO] 4/6/22 1:12:00 PM

Page 28: [9] Deleted Maina, Fadji Zaouna (GSFC-6170)[UNIVERSITY OF MARYLAND  
BALTIMORE CO] 4/6/22 1:12:00 PM

Page 28: [10] Deleted Maina, Fadji Zaouna (GSFC-6170)[UNIVERSITY OF MARYLAND  
BALTIMORE CO] 4/6/22 3:18:00 PM

Page 28: [10] Deleted Maina, Fadji Zaouna (GSFC-6170)[UNIVERSITY OF MARYLAND  
BALTIMORE CO] 4/6/22 3:18:00 PM

Page 28: [10] Deleted Maina, Fadji Zaouna (GSFC-6170)[UNIVERSITY OF MARYLAND  
BALTIMORE CO] 4/6/22 3:18:00 PM

▲  
Page 28: [10] Deleted Maina, Fadji Zaouna (GSFC-6170)[UNIVERSITY OF MARYLAND  
BALTIMORE CO] 4/6/22 3:18:00 PM

▼  
▲  
Page 28: [10] Deleted Maina, Fadji Zaouna (GSFC-6170)[UNIVERSITY OF MARYLAND  
BALTIMORE CO] 4/6/22 3:18:00 PM

▼  
▲  
Page 28: [10] Deleted Maina, Fadji Zaouna (GSFC-6170)[UNIVERSITY OF MARYLAND  
BALTIMORE CO] 4/6/22 3:18:00 PM

▼  
▲  
Page 28: [10] Deleted Maina, Fadji Zaouna (GSFC-6170)[UNIVERSITY OF MARYLAND  
BALTIMORE CO] 4/6/22 3:18:00 PM

▼  
▲  
Page 28: [10] Deleted Maina, Fadji Zaouna (GSFC-6170)[UNIVERSITY OF MARYLAND  
BALTIMORE CO] 4/6/22 3:18:00 PM

▼  
▲  
Page 28: [10] Deleted Maina, Fadji Zaouna (GSFC-6170)[UNIVERSITY OF MARYLAND  
BALTIMORE CO] 4/6/22 3:18:00 PM

▼  
▲  
Page 28: [10] Deleted Maina, Fadji Zaouna (GSFC-6170)[UNIVERSITY OF MARYLAND  
BALTIMORE CO] 4/6/22 3:18:00 PM

▼  
▲  
Page 28: [10] Deleted Maina, Fadji Zaouna (GSFC-6170)[UNIVERSITY OF MARYLAND  
BALTIMORE CO] 4/6/22 3:18:00 PM

Page 28: [10] Deleted Maina, Fadji Zaouna (GSFC-6170)[UNIVERSITY OF MARYLAND BALTIMORE CO] 4/6/22 3:18:00 PM

Page 28: [10] Deleted Maina, Fadji Zaouna (GSFC-6170)[UNIVERSITY OF MARYLAND BALTIMORE CO] 4/6/22 3:18:00 PM

Page 28: [10] Deleted Maina, Fadji Zaouna (GSFC-6170)[UNIVERSITY OF MARYLAND BALTIMORE CO] 4/6/22 3:18:00 PM

Page 28: [10] Deleted Maina, Fadji Zaouna (GSFC-6170)[UNIVERSITY OF MARYLAND BALTIMORE CO] 4/6/22 3:18:00 PM

Page 28: [10] Deleted Maina, Fadji Zaouna (GSFC-6170)[UNIVERSITY OF MARYLAND BALTIMORE CO] 4/6/22 3:18:00 PM

Page 28: [10] Deleted Maina, Fadji Zaouna (GSFC-6170)[UNIVERSITY OF MARYLAND BALTIMORE CO] 4/6/22 3:18:00 PM

Page 29: [11] Deleted Maina, Fadji Zaouna (GSFC-6170)[UNIVERSITY OF MARYLAND BALTIMORE CO] 2/17/22 6:45:00 PM

Page 30: [12] Deleted Maina, Fadji Zaouna (GSFC-6170)[UNIVERSITY OF MARYLAND BALTIMORE CO] 2/18/22 9:56:00 AM

Page 30: [12] Deleted Maina, Fadji Zaouna (GSFC-6170)[UNIVERSITY OF MARYLAND BALTIMORE CO] 2/18/22 9:56:00 AM

Page 30: [12] Deleted Maina, Fadji Zaouna (GSFC-6170)[UNIVERSITY OF MARYLAND BALTIMORE CO] 2/18/22 9:56:00 AM

Page 30: [12] Deleted Maina, Fadji Zaouna (GSFC-6170)[UNIVERSITY OF MARYLAND BALTIMORE CO] 2/18/22 9:56:00 AM

Page 30: [12] Deleted Maina, Fadji Zaouna (GSFC-6170)[UNIVERSITY OF MARYLAND BALTIMORE CO] 2/18/22 9:56:00 AM

Page 30: [12] Deleted Maina, Fadji Zaouna (GSFC-6170)[UNIVERSITY OF MARYLAND BALTIMORE CO] 2/18/22 9:56:00 AM

Page 30: [12] Deleted Maina, Fadji Zaouna (GSFC-6170)[UNIVERSITY OF MARYLAND BALTIMORE CO] 2/18/22 9:56:00 AM

Page 30: [12] Deleted Maina, Fadji Zaouna (GSFC-6170)[UNIVERSITY OF MARYLAND BALTIMORE CO] 2/18/22 9:56:00 AM

Page 30: [12] Deleted Maina, Fadji Zaouna (GSFC-6170)[UNIVERSITY OF MARYLAND  
BALTIMORE CO] 2/18/22 9:56:00 AM

Page 30: [12] Deleted Maina, Fadji Zaouna (GSFC-6170)[UNIVERSITY OF MARYLAND  
BALTIMORE CO] 2/18/22 9:56:00 AM

Page 30: [12] Deleted Maina, Fadji Zaouna (GSFC-6170)[UNIVERSITY OF MARYLAND  
BALTIMORE CO] 2/18/22 9:56:00 AM

Page 30: [12] Deleted Maina, Fadji Zaouna (GSFC-6170)[UNIVERSITY OF MARYLAND  
BALTIMORE CO] 2/18/22 9:56:00 AM

Page 30: [12] Deleted Maina, Fadji Zaouna (GSFC-6170)[UNIVERSITY OF MARYLAND  
BALTIMORE CO] 2/18/22 9:56:00 AM

Page 30: [12] Deleted Maina, Fadji Zaouna (GSFC-6170)[UNIVERSITY OF MARYLAND  
BALTIMORE CO] 2/18/22 9:56:00 AM

Page 30: [12] Deleted Maina, Fadji Zaouna (GSFC-6170)[UNIVERSITY OF MARYLAND  
BALTIMORE CO] 2/18/22 9:56:00 AM

Page 30: [12] Deleted Maina, Fadji Zaouna (GSFC-6170)[UNIVERSITY OF MARYLAND  
BALTIMORE CO] 2/18/22 9:56:00 AM

Page 30: [12] Deleted Maina, Fadji Zaouna (GSFC-6170)[UNIVERSITY OF MARYLAND BALTIMORE CO] 2/18/22 9:56:00 AM

Page 30: [12] Deleted Maina, Fadji Zaouna (GSFC-6170)[UNIVERSITY OF MARYLAND BALTIMORE CO] 2/18/22 9:56:00 AM

Page 30: [12] Deleted Maina, Fadji Zaouna (GSFC-6170)[UNIVERSITY OF MARYLAND BALTIMORE CO] 2/18/22 9:56:00 AM

Page 30: [12] Deleted Maina, Fadji Zaouna (GSFC-6170)[UNIVERSITY OF MARYLAND BALTIMORE CO] 2/18/22 9:56:00 AM

Page 30: [12] Deleted Maina, Fadji Zaouna (GSFC-6170)[UNIVERSITY OF MARYLAND BALTIMORE CO] 2/18/22 9:56:00 AM

Page 30: [12] Deleted Maina, Fadji Zaouna (GSFC-6170)[UNIVERSITY OF MARYLAND BALTIMORE CO] 2/18/22 9:56:00 AM

Page 30: [12] Deleted Maina, Fadji Zaouna (GSFC-6170)[UNIVERSITY OF MARYLAND BALTIMORE CO] 2/18/22 9:56:00 AM

Page 30: [12] Deleted Maina, Fadji Zaouna (GSFC-6170)[UNIVERSITY OF MARYLAND  
BALTIMORE CO] 2/18/22 9:56:00 AM

Page 30: [12] Deleted Maina, Fadji Zaouna (GSFC-6170)[UNIVERSITY OF MARYLAND  
BALTIMORE CO] 2/18/22 9:56:00 AM

Page 30: [12] Deleted Maina, Fadji Zaouna (GSFC-6170)[UNIVERSITY OF MARYLAND  
BALTIMORE CO] 2/18/22 9:56:00 AM

Page 30: [12] Deleted Maina, Fadji Zaouna (GSFC-6170)[UNIVERSITY OF MARYLAND  
BALTIMORE CO] 2/18/22 9:56:00 AM

Page 30: [13] Deleted Maina, Fadji Zaouna (GSFC-6170)[UNIVERSITY OF MARYLAND  
BALTIMORE CO] 2/22/22 10:25:00 AM

Page 30: [13] Deleted Maina, Fadji Zaouna (GSFC-6170)[UNIVERSITY OF MARYLAND  
BALTIMORE CO] 2/22/22 10:25:00 AM

Page 30: [13] Deleted Maina, Fadji Zaouna (GSFC-6170)[UNIVERSITY OF MARYLAND  
BALTIMORE CO] 2/22/22 10:25:00 AM

Page 30: [13] Deleted Maina, Fadji Zaouna (GSFC-6170)[UNIVERSITY OF MARYLAND  
BALTIMORE CO] 2/22/22 10:25:00 AM



Page 30: [13] Deleted Maina, Fadji Zaouna (GSFC-6170)[UNIVERSITY OF MARYLAND BALTIMORE CO] 2/22/22 10:25:00 AM

Page 30: [13] Deleted Maina, Fadji Zaouna (GSFC-6170)[UNIVERSITY OF MARYLAND BALTIMORE CO] 2/22/22 10:25:00 AM

Page 30: [13] Deleted Maina, Fadji Zaouna (GSFC-6170)[UNIVERSITY OF MARYLAND BALTIMORE CO] 2/22/22 10:25:00 AM

Page 30: [13] Deleted Maina, Fadji Zaouna (GSFC-6170)[UNIVERSITY OF MARYLAND BALTIMORE CO] 2/22/22 10:25:00 AM

Page 30: [13] Deleted Maina, Fadji Zaouna (GSFC-6170)[UNIVERSITY OF MARYLAND BALTIMORE CO] 2/22/22 10:25:00 AM

Page 30: [13] Deleted Maina, Fadji Zaouna (GSFC-6170)[UNIVERSITY OF MARYLAND BALTIMORE CO] 2/22/22 10:25:00 AM

Page 30: [13] Deleted Maina, Fadji Zaouna (GSFC-6170)[UNIVERSITY OF MARYLAND BALTIMORE CO] 2/22/22 10:25:00 AM

Page 30: [13] Deleted Maina, Fadji Zaouna (GSFC-6170)[UNIVERSITY OF MARYLAND  
BALTIMORE CO] 2/22/22 10:25:00 AM

Page 30: [13] Deleted Maina, Fadji Zaouna (GSFC-6170)[UNIVERSITY OF MARYLAND  
BALTIMORE CO] 2/22/22 10:25:00 AM

Page 30: [13] Deleted Maina, Fadji Zaouna (GSFC-6170)[UNIVERSITY OF MARYLAND  
BALTIMORE CO] 2/22/22 10:25:00 AM

Page 30: [13] Deleted Maina, Fadji Zaouna (GSFC-6170)[UNIVERSITY OF MARYLAND  
BALTIMORE CO] 2/22/22 10:25:00 AM

Page 30: [13] Deleted Maina, Fadji Zaouna (GSFC-6170)[UNIVERSITY OF MARYLAND  
BALTIMORE CO] 2/22/22 10:25:00 AM

Page 30: [13] Deleted Maina, Fadji Zaouna (GSFC-6170)[UNIVERSITY OF MARYLAND  
BALTIMORE CO] 2/22/22 10:25:00 AM

Page 30: [13] Deleted Maina, Fadji Zaouna (GSFC-6170)[UNIVERSITY OF MARYLAND  
BALTIMORE CO] 2/22/22 10:25:00 AM

Page 31: [14] Deleted Maina, Fadji Zaouna (GSFC-6170)[UNIVERSITY OF MARYLAND  
BALTIMORE CO] 2/22/22 8:57:00 AM

▼  
▲  
**Page 39: [15] Formatted**      **Maina, Fadji Zaouna (GSFC-6170)[UNIVERSITY OF MARYLAND  
BALTIMORE CO]**      **4/6/22 3:36:00 PM**

Font: (Default) Times New Roman, 12 pt, Font color: Black, Pattern: Clear

▲  
**Page 39: [16] Formatted**      **Maina, Fadji Zaouna (GSFC-6170)[UNIVERSITY OF MARYLAND  
BALTIMORE CO]**      **4/6/22 3:36:00 PM**

Font: (Default) Times New Roman, 12 pt, Font color: Black

▲  
**Page 40: [17] Formatted**      **Maina, Fadji Zaouna (GSFC-6170)[UNIVERSITY OF MARYLAND  
BALTIMORE CO]**      **4/6/22 3:36:00 PM**

Font: (Default) Times New Roman, 12 pt, Font color: Black, Pattern: Clear

▲  
**Page 40: [18] Formatted**      **Maina, Fadji Zaouna (GSFC-6170)[UNIVERSITY OF MARYLAND  
BALTIMORE CO]**      **4/6/22 3:36:00 PM**

Font: (Default) Times New Roman, 12 pt, Font color: Black

▲  
**Page 40: [19] Formatted**      **Maina, Fadji Zaouna (GSFC-6170)[UNIVERSITY OF MARYLAND  
BALTIMORE CO]**      **4/6/22 3:36:00 PM**

Font: (Default) Times New Roman, 12 pt, Font color: Black, Pattern: Clear

▲  
**Page 40: [20] Formatted**      **Maina, Fadji Zaouna (GSFC-6170)[UNIVERSITY OF MARYLAND  
BALTIMORE CO]**      **4/6/22 3:36:00 PM**

Default Paragraph Font, Font: (Default) Times New Roman, 12 pt, Font color: Black

▲